



Refitting the Context: A Reconsideration of Cultural Change among Early *Homo sapiens* at Fumane Cave through Blade Break Connections, Spatial Taphonomy, and Lithic Technology

Armando Falcucci¹ · Domenico Giusti² · Filippo Zangrossi^{3,4} · Matteo De Lorenzi⁵ · Letizia Ceregatti⁵ · Marco Peresani^{5,6}

Accepted: 3 December 2024

© The Author(s) 2024

Abstract

High-resolution stratigraphic frameworks are crucial for unraveling the biocultural processes behind the dispersals of *Homo sapiens* across Europe. Detailed technological studies of lithic assemblages retrieved from multi-stratified sequences allow archaeologists to precisely model the chrono-cultural dynamics of the early Upper Paleolithic. However, it is of paramount importance to verify the integrity of these assemblages before building explanatory models of cultural change. In this study, multiple lines of evidence suggest that the stratigraphic sequence of Fumane Cave in northeastern Italy experienced minor post-depositional reworking, establishing it as a pivotal site for exploring the earliest stages of the Aurignacian. By conducting a systematic search for break connections between blade fragments and applying spatial analysis techniques, we identified three well-preserved areas of the excavation containing assemblages suitable for renewed archaeological investigations. Subsequent technological analyses, incorporating attribute analysis, reduction intensity, and multivariate statistics, have allowed us to discern the spatial organization of the site during the formation of the Protoaurignacian palimpsest A2–A1. Moreover, diachronic comparisons between three successive stratigraphic units prompted us to reject the hypothesis of techno-cultural continuity of the Protoaurignacian in northeastern Italy after the onset of the Heinrich Event 4. Based on the variability of the lithic and osseous artifacts, the most recent assemblage analyzed, D3b alpha, is now ascribed to the Early Aurignacian, aligning the evidence from Fumane with the current understanding of the development of the Aurignacian across Europe. Overall, this study demonstrates the high effectiveness of the break connection method when combined with detailed spatial analysis and lithic technology, providing a methodological tool particularly amenable to be applied to sites excavated in the past with varying degrees of recording accuracy.

Keywords Protoaurignacian · Early Aurignacian · Lithics · Refittings · Assemblage integrity · Spatial analysis · Italy

Armando Falcucci
armando.falcucci@uni-tuebingen.de

¹ Department of Geosciences, Prehistory and Archaeological Sciences Research Unit, Eberhard Karls University of Tübingen, Tübingen, Germany

² Paleoanthropology, Senckenberg Centre for Human Evolution and Paleoenvironment, University of Tübingen, Tübingen, Germany

³ Department of History and History of Art, University Rovira i Virgili, Avinguda de Catalunya 35, 43002 Tarragona, Spain

⁴ Catalan Institute of Human Paleoecology and Social Evolution (IPHES-CERCA), Zona Educacional 4, Campus Sescelades URV (Building W3), 43007 Tarragona, Spain

⁵ Department of Humanities, Prehistoric and Anthropological Sciences Unit, University of Ferrara, Ferrara, Italy

⁶ Institute of Environmental Geology and Geoengineering, National Research Council, Milan, Italy

Introduction

Prehistoric archaeologists rely on interdisciplinary analyses of multi-stratified sites to reconstruct past environments, climate fluctuations, population dynamics, and related cultural changes. One of the most powerful tools for modeling chrono-cultural changes is the techno-typological study of lithic artifacts retrieved from well-dated, geo-archaeologically defined layers. Lithics, the most common findings in Paleolithic contexts, represent the byproducts of learned behaviors. These artifacts allow for discussions on the nature and mode of acquisition of new technologies by foraging groups, thanks to detailed technological and typological assessments (Tostevin, 2013). However, to fully understand cultural changes, it is crucial to understand the depositional and post-depositional history of the archaeological record as much as possible. This can be achieved by discerning and modeling the natural and anthropogenic processes that shaped and preserved the stratigraphic sequence (e.g., Butzer, 1982; Schiffer, 1987; Texier, 2000).

A rigorous analysis of site formation processes is particularly critical in karstic cave sites (Deschamps & Zilhão, 2018; Farrand, 2001; Goldberg et al., 1993; Villa & Courtin, 1983). Unlike open-air sites, cave sites present unique characteristics in terms of syn- and post-depositional processes (Barton & Clark, 1993; Hughes & Lampert, 1977). Caves are frequently subject to water runoff, freeze-thaw cycles, rockfalls, massive sedimentary collapses, and animal burrowing (Texier, 2000). The cumulative effects of these processes can result in the erosion of parts of the archaeological deposit, leading to hiatuses and unconformities in the stratigraphic sequence. Additionally, the confined living conditions in caves and rock shelters suggest repeated use of the same area over various periods, resulting in intricate palimpsest formations (Bailey, 2007), particularly when sedimentation rates are slow. In recent years, several studies have made significant advances in addressing these complex issues (Bel, 2022; Bel et al., 2020; Deschamps & Zilhão, 2018; Thomas et al., 2019).

On top of that, archaeologists often face the challenging task of determining whether the stratigraphic layers identified during site excavation—based on sedimentological, geological, and archaeological observations—are truly meaningful for analyzing cultural diachronic changes (Boschian et al., 2017). Unfortunately, these stratigraphic layers are frequently used to model cultural variability without thorough prior evaluation (Romagnoli et al., 2018). A noteworthy study on the Châtelperronian site of Cassenade in southwestern France rigorously addresses this critical issue (Discamps et al., 2023). At Cassenade, distinct human and carnivore occupations were found to

be mixed within the same layers originally defined during fieldwork. In this context, sedimentation rate emerges as a crucial factor influencing the ability to identify sub-layers, anthropogenic features, and discrete events within palimpsest formations. This issue is exacerbated at sites excavated using low-resolution techniques, such as inaccurately documenting the absolute elevation of archaeological finds (McPherron et al., 2005), or at sites investigated with varying excavation strategies over time (Gravina et al., 2018).

In the early Upper Paleolithic, achieving the highest possible resolution in modeling cultural change dynamics is crucial, especially for sites with thick stratigraphic sequences. During this period, technocomplexes generally exhibit faster rates of diachronic change and intermittent regionalization, likely linked to varying degrees of population interconnectivity (Maier et al., 2022). The Aurignacian stands out as the first Upper Paleolithic technocomplex with a broad geographic distribution (Le Brun-Ricalens & Bordes, 2007), contrasting with more regionally localized and debated technocomplexes like the Uluzzian (Moroni et al., 2018; Peresani et al., 2019b) and the Châtelperronian (Pelegrin, 1995; Roussel et al., 2016).

The earliest manifestations of the Aurignacian, dating to ~43–40 ka cal BP (Frouin et al., 2022; Higham et al., 2009; Nigst et al., 2014; Wood et al., 2014), have been pivotal in understanding human adaptive responses to diverse ecological settings and changing environments (Anderson et al., 2015; Banks et al., 2013a; Giaccio et al., 2017; Le Brun-Ricalens & Bordes, 2007). The observed diachronic variability in both lithic and bone tools has enabled archaeologists to identify distinct chrono-cultural phases within the Aurignacian, with extensive research in southwestern France playing a key role in this task (Anderson et al., 2018). This chrono-cultural model, initially based on sites in southwestern France, has since been adopted on a pan-European scale (Dinnis et al., 2019; Teyssandier & Zilhão, 2018).

Some scholars have argued that the Aquitaine model cannot be uncritically applied to such a broad geographic framework (Bataille et al., 2018; Falcucci et al., 2020; Genain, 2021). One key site for discussing Aurignacian chrono-cultural dynamics outside of southwestern France is Fumane Cave in northeastern Italy (Fig. 1a,b). Fumane contains a stratigraphic sequence spanning most of the Aurignacian's chronological range, from ~41 ky cal BP to the onset of Heinrich Event 3 (Higham et al., 2009; Peresani, 2022). Detailed techno-typological studies of the entire Aurignacian sequence have revealed a remarkable similarity among the investigated layers, leading Falcucci et al. (2020) to propose that the Protoaurignacian in northeastern Italy persisted longer than in regions like southwestern France and northern Iberia.

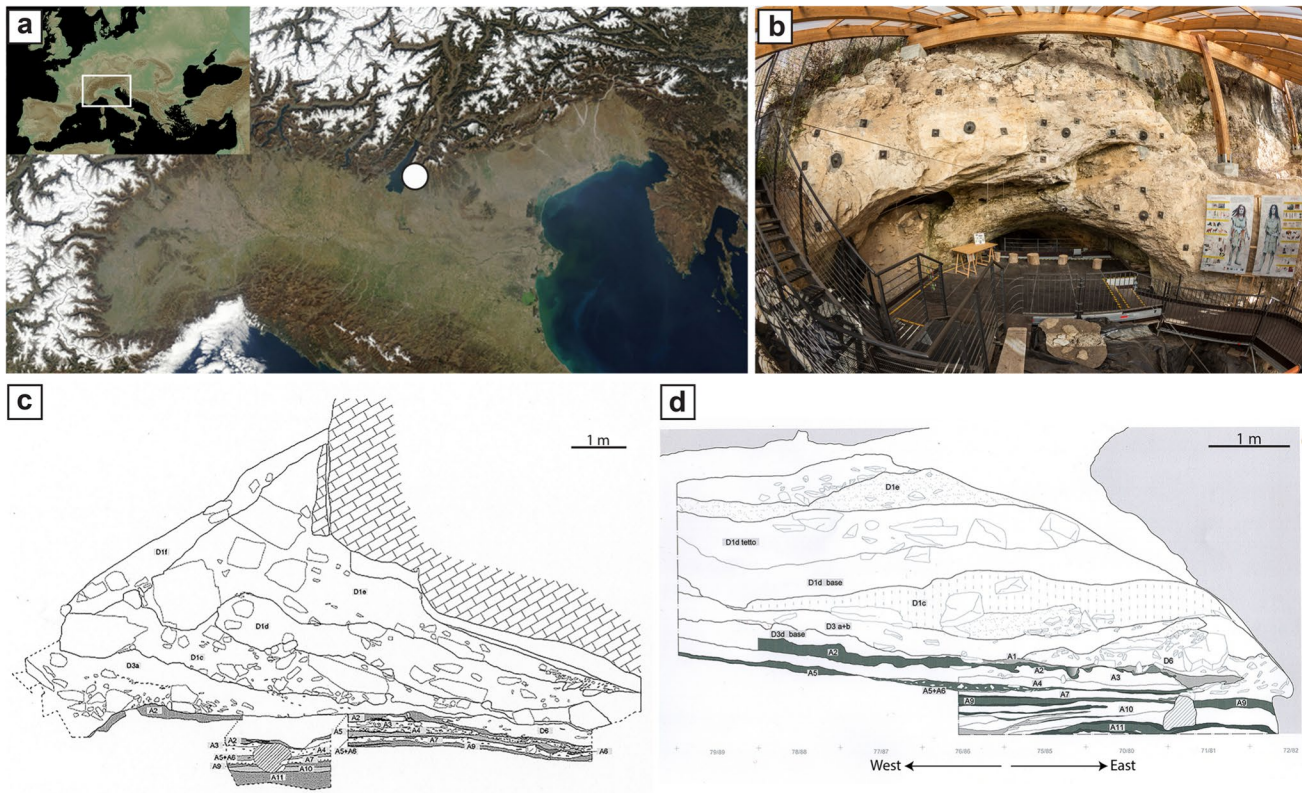


Fig. 1 **a** Physical map of Europe showing the geographical location of Fumane Cave (indicated by a white dot) in northeastern Italy; **b** View of the site's entrance with Tunnel B forming the main cavity, and Tunnel A on the left. Tunnel C is located on the right side of the cave but is not visible in the image. For a plan view of the cave, see the sketch in Fig. 2; **c** Sketch of the sagittal section of the cave, showing evidence of late Mousterian (A11–A4), Uluzzian (A3), Aurignacian (A2–A1, D6–D3), and the stratigraphic complex D1; **d** Sketch of the transversal section of the cave, depicting the succession of SUs mentioned above. The base of D3 is more visible in section (c). See also SM Figs. S1 and S2 for photographs of the stratigraphic profiles (Section c by M. Cremaschi and M. Peresani, redrawn by S. Muratori; section d by M. Peresani and S. Muratori)

nacian (A2–A1, D6–D3), and the stratigraphic complex D1; **d** Sketch of the transversal section of the cave, depicting the succession of SUs mentioned above. The base of D3 is more visible in section (c). See also SM Figs. S1 and S2 for photographs of the stratigraphic profiles (Section c by M. Cremaschi and M. Peresani, redrawn by S. Muratori; section d by M. Peresani and S. Muratori)

However, Falcucci et al. (2020) relied solely on field notes and photographic documentation to assess the varying degrees of post-depositional disturbances across different cave sectors and to evaluate the reliability of the stratigraphic sequence documented during the excavations. Similarly, the proposed stratigraphic correlations among different excavation areas were mainly based on find density and the excavation history of the site. This approach is problematic, as previous studies have suggested stratigraphic issues at Fumane due to the heterogeneous charcoal content in A2 and the presence of dates that were not in stratigraphic order above it (Banks et al., 2013a, b; Zilhão et al., 2024). Additionally, artifacts diagnostic of the Early Aurignacian, such as split-based points, were recovered, further complicating the stratigraphic and chrono-cultural interpretation (Teyssandier & Zilhão, 2018).

In this study, we build on the previous work by evaluating the deposit's integrity using for the first time a lithic taphonomic approach and in-depth spatial analyses. Lithic taphonomy is a powerful tool for unraveling the formation processes of archaeological sites and assessing the integrity

of lithic assemblages (Romagnoli & Vaquero, 2019; Sisk & Shea, 2008; Villa, 2004), effectively supplementing geoarchaeological data. To test the hypothesis of cultural continuity across Fumane Cave's Aurignacian sequence and assess the integrity of the assemblages, we employ the blade break connection method by Bordes (2000), complemented by a comprehensive spatial analysis of conjoining links.

Unlike technological refits (Romagnoli & Vaquero, 2019 and references therein), break connections among lithic fragments offer deeper insights into the natural and human processes responsible for the formation of the archaeological record. Additionally, this approach systematically tests all potential connections (Bel et al., 2020; Cziesla, 1987; Gravina et al., 2018). The method assumes that blades primarily break in place due to various processes (e.g., knapping mistakes, tool manufacturing, trampling, and sediment compression). A significant number of connections in spatial proximity would suggest minimal syn- and post-depositional processes, while connections between distant areas would indicate displacement caused by either more intense

post-depositional disturbances or complex processes, including anthropogenic ones. For instance, Paleolithic foragers might have accumulated lithics in various cave areas as part of refuse disposal strategies (Bel et al., 2020). Alternatively, artifacts could have been vertically displaced due to household activities, such as digging pits for combustion features.

By applying the break connection method to the Aurignacian sequence of Fumane Cave, we aim to address four key questions: Firstly, we will determine the extent to which post-depositional events influenced the formation of the Aurignacian lithic assemblages. Secondly, we will critically evaluate the cultural significance of the stratigraphic units (SUs) defined during excavations and the accuracy of the previously proposed stratigraphic correlations. Thirdly, we will assess the intra-site variability and spatial organization of the site by studying different cave areas that appear to be less affected by inter-SU artifact migration or excavation inaccuracies. Lastly, we will test the hypothesis of local chrono-cultural continuity of the Protoaurignacian (Falcucci et al., 2020) through a diachronic analysis using those excavation areas and SUs with higher intra-SU conjoining rates. Through these four objectives, our overarching aim is to refine our understanding of the Aurignacian's chrono-cultural development on a regional scale, thereby contributing to a deeper comprehension of human cultural dynamics during the early Upper Paleolithic.

Materials and Methods

Excavation Protocol and Selection of the Analytical Units

Fieldwork at Fumane has spanned several decades, employing various excavation methods, protocols, and inconsistent digital registration techniques (see Supplementary Material; SM Note S1). The primary excavations targeting the Upper Paleolithic deposits occurred between 1988 and 2006. In most cases, SUs were defined based on geoarchaeological criteria and archaeological content. However, when stratigraphic boundaries were unclear, excavations proceeded by removing spits of sediment. This approach led to varying degrees of accuracy in the definition of SUs. Additionally, the characteristics of the SUs vary in different areas of the excavation and not all SUs were identified across the entire excavation area, primarily due to the significant differences in sedimentary composition. Consequently, the extension and composition of the SUs are not uniform, with some SUs displaying substantial lateral variation, complicating straightforward archaeological correlations. SM Note S2 provides a detailed description of all studied SUs, with a focus on sediment composition, evidence of anthropogenic features, major post-depositional events identified during

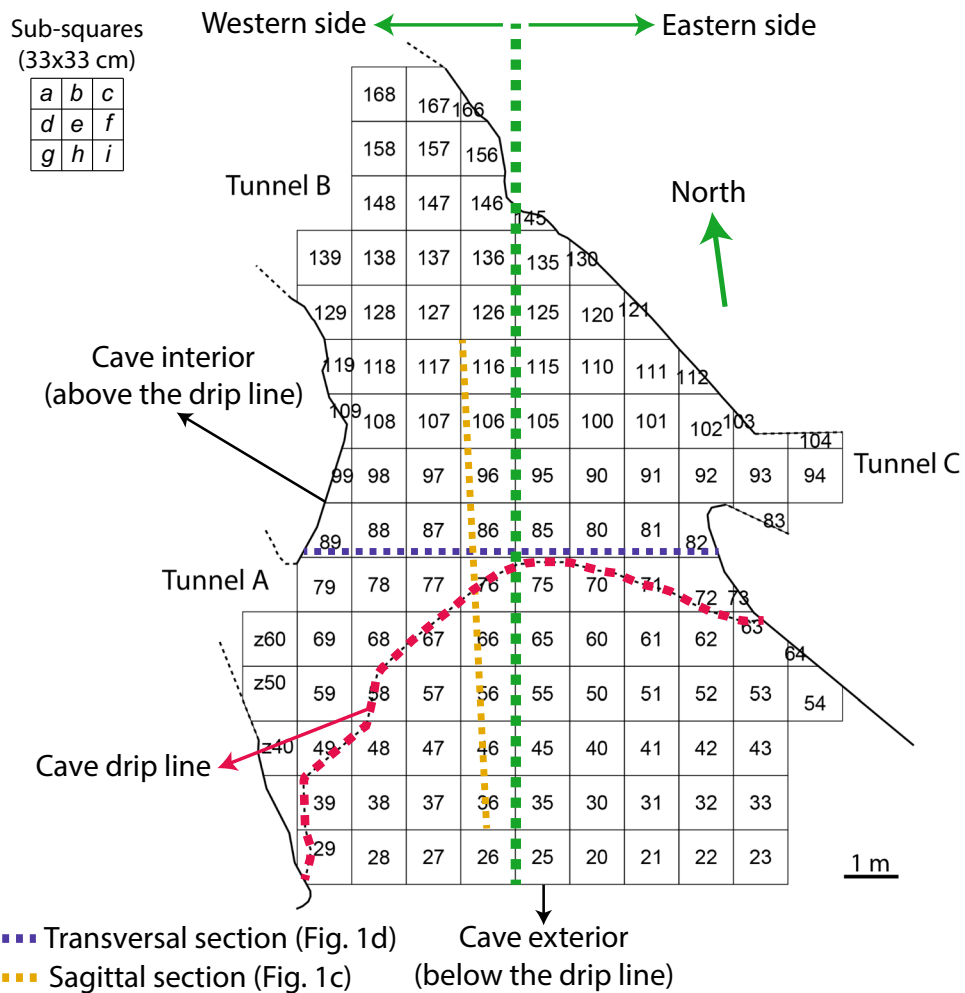
excavations, and spatial extent. This thorough description is based on an extensive study of all available documentation, including fieldwork notebooks, drawings, and photographic archives (see also SM Figs. S1–S13).

Excavations at Fumane followed a square-meter grid system (Fig. 2). SUs were excavated in sub-squares of 33×33 cm (labeled from *a* to *i*, from top to bottom in alphabetical order), allowing for the plotting of most finds within this spatial framework. However, the systematic piece-plotting of individual artifacts did not become standard practice until 1996. Nevertheless, the extension and elevation of SUs were documented throughout the excavation period. From the outset, systematic wet sieving of excavated sediment was conducted to recover the smallest organic and inorganic artifacts. This practice was only partially followed in the initial years when excavating the éboulis of the upper sedimentary complex in the southeastern portion of the cave, where sediments were relatively poor in archaeological content. During these initial years, excavation progressed at a relatively high pace to uncover the rich Protoaurignacian SU A2 and gain access to the cave's interior.

From 1996 onward, excavations expanded to the westernmost part of the cave, where more fine-grained methods were applied, leading to a better understanding of the SUs forming the D3 sequence. This has made it difficult to establish explicit correlations between the western and eastern sections of the cave. For example, SU D3b alpha was not documented in the eastern part of the cave. This may be attributed to either the coarser excavation methods used in the D3 complex before 1996 or the increased stoniness of the SUs in that area, which may have obscured or prevented the preservation of this thin SU. Additionally, the interplay between excavation history and the stark difference in sediment composition between the eastern and western sectors of the cave has resulted in the identification of distinct SUs that may not be stratigraphically consecutive but are instead separated by an abrupt transition, roughly corresponding to the boundary between the micritic banks and the calcarenites characteristic of the cave (see also SM Note S2 for more details). One of the aims of the break connection program presented in this work is to address this issue, along with testing the integrity of the lithic assemblages.

In this study, we considered a total of 15 SUs, spanning from the earliest Protoaurignacian to the uppermost SUs of the stratigraphic sequence: A2, A2R, A1, D6, D3d base, D3d, D3b alpha, D3b, D3a, D3 + D6, D3a + b sabbie, D3a + b, D1c, D1d, and D1e. Except for the early Gravettian assemblage from SU D1d (Falcucci & Peresani, 2019) and the semi-sterile D1e, all other SUs yielded lithic assemblages related to the Aurignacian technocomplex. Several studies have analyzed these SUs, focusing on lithic industries (Bertola et al., 2013; Broglio et al., 2005; Falcucci et al., 2020), the zooarchaeological record and the organic

Fig. 2 Plan view of the cave showing its three main tunnels (A, B, and C) and the square meter grid used during the archaeological excavation, along with the division of the site according to the cave drip line and orientation. The figure also highlights the locations of the stratigraphic profiles depicted in Fig. 1c (sagittal section) and Fig. 1d (transversal section). Additionally, the visualization includes the subdivision of square meter units into 33×33 cm sub-squares (top left)



tools (Broglio & Dalmeri, 2005; Gurioli et al., 2005; Marín-Arroyo et al., 2023), and the symbolic artifacts (Peresani et al., 2019a; Sigari et al., 2022).

Lithic Break Connection Program

In previous decades, the analysis of the Upper Paleolithic assemblages from Fumane Cave primarily relied on the SUs defined during fieldwork to investigate the site's chrono-cultural development. To address the limitations of this approach and assess the integrity of the studied lithic assemblages, we employed a lithic break connection method (Bordes, 2000). In the literature, the terms "break connection" and "conjoin" are used interchangeably, and we will use both terms throughout this paper. This method allows for the objective quantification of intra- and inter-SU connections by systematically testing all potential connections between recovered fragments. Initially refined by Bordes (2000), this technique has been widely applied to Upper Paleolithic industries characterized by a strong laminar component (Bel et al., 2020; Bordes, 2002; Tsanova,

2008). More recently, it has also been tested, with less success, on flake-dominated assemblages (Gravina et al., 2018).

For this study, we focused exclusively on blade fragments, as the Aurignacian assemblages at Fumane are known for their significant laminar component (Falcucci et al., 2020). Based on Gravina et al. (2018), flake fragments are generally more challenging to connect. We selected all blade fragments with a width of 12 mm or greater from 15 SUs across the entire excavation area. Due to their fragmented state, these blades could not be classified by their standard metric definition (i.e., length at least twice the width). Instead, they were categorized based on morphological and technological attributes, such as edge regularity, presence of small butts and lips, and unidirectional sub-parallel to convergent dorsal scars. Bladelets (i.e., laminar blanks with a width under 12 mm; Tixier, 1963) were excluded from this study to optimize the search for break connections, given the already substantial number of blade fragments. However, Bel et al. (2020) have demonstrated that the method can also be successfully applied to small-sized laminar implements.

Approximately 400 person-hours were required to prepare the assemblages for the systematic break connection program. During this preparatory phase, we categorized and quantified all fragments based on their preservation (i.e., proximal, mesial, and distal), raw material type, presence of cortex coverage, and localization of retouch. A small number of proximal fragments with hinged terminations, indicative of knapping errors resulting in the detachment of an already fragmented blade (Inizan et al., 1995), were excluded from the analysis. The total sample size comprised 3254 blade fragments (Table 1), making it the largest sample ever analyzed using this method. Proximal portions were the most common, followed by distal and mesial fragments. These fragments were distributed across all analyzed SUs, with the highest frequency found in SU A2. Variations in fragment numbers are consistent with overall artifact density within each SU (Falcucci et al., 2017, 2020). This numerical disparity in lithic assemblages can be attributed to factors such as the rapid sedimentation rate of the younger sequence, progressive deterioration of the cave walls, and reduced frequency of cave use after the deposition of SUs A2–A1 (Falcucci et al., 2020).

The fragments were organized and laid out on five tables, each measuring 250 × 90 cm (total area: 11.25 m²), following a precise raw material and techno-typological sorting strategy (SM Fig. S14). All possible combinations

were systematically tested, including connections between proximal, mesial, and distal fragments, as well as mesial-to-mesial and mesial-to-distal connections. In cases where thermally altered blades could not be assigned to a specific raw material variety, fragments were tested against all raw material types. Cortical blades were also tested with non-cortical fragments when the cortex did not reach the fracture. Tests were conducted both intra- and inter-SU, beginning with spatially related square meters and gradually extending to more distant sectors of the cave. Three researchers (AF, FZ, MDL) collectively dedicated approximately 300 working hours to the break connection program, meticulously double-checking all possible combinations to enhance the conjoining rate. MP and two colleagues occasionally contributed to this work, identifying additional connections. Each possible combination was tested at least twice. Connection tests were then halted only when the trade-off between costs (i.e., time) and benefits (i.e., number of joins) significantly decreased, essentially reaching the point of diminishing returns (Laughlin & Kelly, 2010). A total of 509 connecting blade fragments were identified, forming 247 complete blades.

All break connections found and analyzed in this study were recorded in a spreadsheet, documenting the square and SU of provenance, metric attributes (i.e., length, width, and thickness), and taphonomic traits (e.g., thermal alterations). Fracture types were not systematically documented, as most fragments displayed bending fractures, which can result from various factors, including post-depositional processes like trampling, as well as knapping and breakage during use (Cotterell & Kamminga, 1987; Eren et al., 2010; Fischer et al., 1984; Jennings, 2011; Roche & Tixier, 1982). Conjoining rates were calculated for the entire sample and each SU, based on the total number of fragments tested and those successfully connected (Cziesla, 1990), as follows:

$$\frac{\text{Number of successfully connected fragments}}{\text{Total number of fragments tested}} \times 100$$

Intra- and inter-SU conjoining rates were then compared to assess the significance and extent of artifact displacement.

Spatial Analysis

The results of the break connection program were further evaluated through a comprehensive spatial analysis of the horizontal and vertical distributions, the extension and direction of connection lines, areal counts, and the areal ratio between different subsets of data. To conduct these spatial analyses, we first undertook a thorough re-evaluation of all excavation documentation, including fieldwork notebooks, plan views, stratigraphic sections, and photographic material. Additionally, we reviewed and digitized all past

Table 1 Classification of the blades used in this study according to fragment preservation and stratigraphic unit (SU) of provenience (from the lowermost SU A2 to the top of the stratigraphic sequence in SU D1e)

	Proximal	Mesial	Distal	Total
SU	n (%)	n (%)	n (%)	n (%)
D1e	1 (50%)	1 (50%)	0 (-)	2 (0.1%)
D1d	2 (40%)	0 (-)	3 (60%)	5 (0.2%)
D1c	6 (33.3%)	7 (38.9%)	5 (27.8%)	18 (0.6%)
D3a+b	22 (39.3%)	18 (32.1%)	16 (28.6%)	56 (1.7%)
D3a+b sabbie	6 (28.6%)	5 (23.8%)	10 (47.6%)	21 (0.6%)
D3+D6	39 (28.3%)	47 (34.1%)	52 (37.7%)	138 (4.2%)
D3a	0 (-)	0 (-)	2 (100%)	2 (0.1%)
D3b	25 (39.7%)	15 (23.8%)	23 (36.5%)	63 (1.9%)
D3b alpha	31 (44.3%)	22 (31.4%)	17 (24.3%)	70 (2.2%)
D3d	18 (32.7%)	16 (29.1%)	21 (38.2%)	55 (1.7%)
D3d base	82 (40.4%)	51 (25.1%)	70 (34.5%)	203 (6.2%)
D6	95 (41.1%)	61 (26.4%)	75 (32.5%)	231 (7.1%)
A1	280 (39.9%)	184 (26.2%)	237 (33.8%)	701 (21.5%)
A2R	49 (30.1%)	46 (28.2%)	68 (41.7%)	163 (5%)
A2	585 (38.3%)	435 (28.5%)	506 (33.2%)	1526 (46.9%)
Total	1241	908 (27.9%)	1105 (34%)	3254 (100%) (38.1%)

The last column sums the overall number of fragments within each SU. Percentages are provided in brackets

databases of piece-plotted artifacts, correcting handwritten coordinates as needed. This extensive digitization and data cleaning process allowed us to build a consistent spatial database of the lithic assemblage and gain a clearer understanding of the relative spatial extensions of the SUs.

Regarding our sample of break connections, only a small number of connected blade fragments (32 out of 509) had unique 3D spatial coordinates recorded during the most recent excavations. For the remaining fragments ($n=477$), X and Y coordinates were extrapolated, when possible, from the central coordinates of the sub-square (or square, if sub-square information was lacking) of provenance for each fragment. The coordinates were then randomized within the spatial limits of the corresponding sub-square or square, following common practices in the field (e.g., Giusti et al., 2018; Sánchez-Romero et al., 2022). Only three fragments from D6 could not be spatially located due to a lack of information on their square of origin and were therefore excluded from subsequent spatial analyses.

For the Z coordinates of the non-plotted fragments, we used a combination of two approaches. The first approach utilized the mean Z coordinate of all plotted pieces from the same square of origin as the non-plotted and sieved fragment. This method provided estimated elevations for 107 out of 474 fragments. The second approach relied on the average Z elevation of the SU of provenance, as recorded in the square or sub-square of origin. This method provided estimated elevations for an additional 357 fragments. Elevation values were then randomized within the range of maximum and minimum Z values for the reference SU in the square or sub-square of origin. In total, out of our sample of 509 connections from 12 SUs, XY coordinates could be modelled for 506 fragments and XYZ coordinates could be modelled for 496 fragments. The fragments excluded from the analyses were all from SUs D6 ($n=10$) and D3 + D6 ($n=3$).

To address our research questions, we adopted a multi-pronged spatial analytic approach, analyzing both intra- and inter-SU connections. We analyzed (1) the length of conjoining lines; (2) their vertical extension; (3) their orientation patterns; (4) the distribution of observed thermal alterations on those conjoined fragments; (5) the areal ratio between the densities of blade fragments and complete blades. We dubbed this ratio the standardized fracture ratio (SFR) and used it as an indication of the relative risk of occurrence of fractures in the blade assemblage.

Length of Conjoining Lines

Horizontal distances among connected fragments were classified into four categories defined by Cziesla (1990): short (<0.5 m), medium (0.5–2.1 m), long (2.1–4 m), and very long (>4 m) distances. These length classes were then analyzed by the number of connections (2, 3, or 4 connected

fragments). According to Cziesla (1990), a prevalence of short connections is considered a proxy for a well-preserved archaeological record, with shorter lines indicating minimal reworking processes and greater relevance for behavioral studies. We expect shorter connections to be more frequent within single SUs (intra-SU). Conversely, long or very long lines may indicate significant material dispersion, potentially due to prolonged settlement, post-depositional processes, human or animal trampling, organized use of space, or karstic processes like gravity or water runoff. Longer connections are expected to be more frequent between different SUs (inter-SU).

Vertical Extension of Conjoining Lines

Using the subset of 496 connecting fragments, we calculated the absolute vertical distance (ΔZ) between pairs of connected fragments. These ΔZ values were grouped by length classes (Cziesla, 1990), for both intra- and inter-SU connections. Lower ΔZ values are anticipated in the short-length class, while higher values are progressively expected in longer connections. We assume that higher ΔZ values are more likely to occur in inter-SU connections (Villa, 1982).

Orientation of Conjoining Lines

The orientation of conjoining lines, often analyzed in technological studies, serves as a proxy for natural or behavioral processes (Discamps et al., 2023; Vaquero et al., 2017; among others). In the context of a lithic break connection program, orientation patterns can also indicate taphonomic or cultural processes. Here, we evaluated orientation patterns for a subset of 87 intra-A2 connections composed of 2 fragments, which constitute the majority of the intra-SU subsample ($n=128$). We also analyzed the intra-A1 connections ($n=20$), the subset of A2/A1 inter-SU connections ($n=27$), and the subset of long and very long connections in A2 and A1. Rose diagrams were used to visualize the distribution of line directions on the horizontal plane, while Benn diagrams (Benn, 1994) were employed to compare different datasets in three-dimensional space. The Benn diagram distinguishes between linear (clustered), planar (girdle), or isotropic distributions. Although no published orientation datasets from other break connection programs are available, the Benn diagram was used here primarily to characterize the orientation patterns relative to the studied SUs.

Distribution of Thermal Alterations

We visually analyzed the spatial distribution of thermal alterations in two subsets of connected fragments (intra-A2 and inter-A2/A1), considering the distribution of anthropogenic features identified during excavations (Broglio et al., 2006) and

partially analyzed by Marcazzan et al. (2022), using microcontextual geo-archaeological techniques.

Standardized Fracture Ratio (SFR)

To provide a comprehensive, diachronic context to the spatial distribution of connected blade fragments, we examined the relative spatial distribution of blade fragments compared to complete blades from corresponding SUs. Drawing on methods used in spatial epidemiology (Diggle, 2003; Gatrell et al., 1996), we treated blade fragments as “cases” and complete blades as “controls”. The spatial distribution of cases represents different processes leading to blade breakage (e.g., sediment compression, trampling, intentional breaking), while controls refer to complete blades. Mapping cases alone gives no information about the “risk” of their occurrence (i.e., the risk of a fracture occurring), given that the cases are mainly distributed according to the underlying record (i.e., controls). A common method used in spatial epidemiology to overcome such a limit relies on the estimation of the “risk”, in a given region i , as the ratio between the number of observed cases (O) in region i (square, sq) and stratum j (stratigraphic unit, SU) and a Poisson distribution, namely the expected number of cases (E), with mean equal to the number of controls in region i and stratum j . Such a ratio is known in spatial epidemiology as the standardized mortality ratio (SMR; Bivand et al., 2013).

Following Bivand et al. (2013), the standardized fracture ratio (SFR) can be defined as $SFR_i = O_i/E_i$ with O_i as the number of blade fragments in sq_i and SU_j (observed cases) and E_i as the number of complete blades in sq_i and SU_j (expected cases). Thus, it would be of special interest the region i where the relative risk (SFR) is significantly higher than 1. A significantly higher density of blade fragments with respect to the expected complete blades would suggest that e.g., a process leading to the break of the blades was more intense in region i than other regions; or a process selectively accumulated blade fragments in region i more than other regions. To grasp the local risk of blade breaks happening in such a dynamic environment provides further insights into the full understanding in taphonomic terms of a lithic break connection program. To gain additional detail, we also calculated a modified SFR that, for observed cases, used only the fragments involved in short and medium distance connections. If the SFR significantly exceeds 1, it may indicate a localized process or a combination of processes that caused in-place blade breakage without significant fragment dispersion.

Technological and Chrono-Cultural Reassessment of the Aurignacian Assemblages

We reassessed the technological and chrono-cultural variability of the Aurignacian lithic assemblages at Fumane, focusing on the SUs and excavation areas identified as most

suitable based on our spatial analyses. For this purpose, we sampled the techno-typological datasets, previously compiled by one of us (AF), by SU and square meter of provenance. The new technological analysis of the selected areas and SUs employed a combination of attribute analysis (Andrefsky, 1998) and reduction sequence analysis (Inizan et al., 1995), following the methodologies established in prior studies at the site.

Our analysis explored both intra- and inter-SU variability concerning raw material selection strategies, core reduction patterns, reduction intensity proxies, and the frequency of cores and other diagnostic tools associated with initial phases of the Aurignacian, specifically the Protoaurignacian and Early Aurignacian. This technological analysis was further complemented by the quantification of osseous tools and personal ornaments recovered from the selected areas and SUs. The presence and characteristics of bone tools and ornaments are essential when investigating the chrono-cultural development of the Aurignacian. Osseous tools have been extensively described in previous studies (Bertola et al., 2013; Broglio & Dalmeri, 2005, among others), while the classification of marine and freshwater shells follows the work of Peresani et al. (2019a).

The primary focus of our reassessment was on the variability of blade and bladelet production, which are defining characteristics of the Aurignacian technocomplex. We utilized discrete and metric attributes previously compiled by Falcucci et al. (2017) and Falcucci et al. (2020). Core types were categorized according to the classification system proposed by Falcucci and Peresani (2018), and the typological list used was a revised and simplified version of widely recognized Upper Paleolithic typologies (de Sonneville-Bordes, 1960; Demars & Laurent, 1992). Additionally, we incorporated supplementary data derived from 3D models of cores published by Falcucci and Peresani (2023). By applying the scar density index (SDI) on the 3D models of all blade and bladelet cores, following the method developed by Clarkson (2013), we explored variations in reduction intensity across the lithic subsets. The SDI was calculated by measuring the core surface area (in mm^2) and counting all visible scars longer than 20 mm, as outlined by Lombao et al. (2023). The core surface area was then divided by the total number of visible scars to obtain the SDI, which was subsequently logarithmically transformed (LogSDI).

To highlight differences between various data subsets, we employed univariate non-parametric statistical methods on both metric and categorical variables. Additionally, we conducted a multiple correspondence analysis (MCA) to examine several interrelated variables associated with the technological and morphometric features of bladelets (Cascalheira, 2019; Leplongeon et al., 2020; Scerri et al., 2014). The MCA allowed us to reduce the complexity of our data

and explore correlations between different variables. Furthermore, we used K-means clustering algorithms to categorize morphological continuous variables, such as blank elongation and robustness, following Cascalheira's (2019) approach. Categories representing less than 5% were condensed into a single category labeled "Other." Using the scores and loadings obtained from the MCA, we assessed the statistical differences between assemblages through an analysis of variance (ANOVA), providing insights into the technological and chronological nuances of the Aurignacian assemblages.

Results: Part One

Quantification of the Break Connections

We successfully connected 509 out of 3254 blade fragments, yielding an overall conjoining rate of 15.6%. These connections encompass a total of 247 blades, with the majority involving two fragments ($n=234$), while connections with three ($n=11$) or four ($n=2$) fragments are less common (Fig. 3). The number of connections identified varies across the stratigraphic sequence, with the highest concentrations found in the lowermost SUs A2 and A1 (Table 2). Interestingly, these SUs also had the highest number of blade fragments (1526 and 701, respectively), which aligns with the overall density of lithic materials previously reported by Falcucci et al. (2020). However, it is important to note that conjoining rates do not strictly correlate with the number of available fragments. For instance, despite the lower frequency of fragments in SUs such as A2R, D6, D3 + D6, D3d base, D3d, and D3b alpha, these SUs exhibit higher conjoining rates than A1. Conversely, SUs with fewer blade fragments show very low conjoining rates. For example, no connections were found in D1e, D1d (early Gravettian), and D3a, which will therefore be excluded from the subsequent spatial analysis. Overall, SUs A2, D3d, and D3b alpha stand out for their higher conjoining rates, each exceeding 18%.

The majority of intra-SU connections are found in A2 ($n=188$), followed by A1 ($n=42$). Intra-SU connections exceed 50% only in SUs A2, A1, D3b alpha, and D3 + D6. Inter-SU connections, however, are common across the site, with an overall percentage of 45.2%. These connections are particularly frequent in SUs from the upper complex D, where, for instance, only inter-SU connections were identified in SUs D3d, D3a+b, D3a+b sabbie, and D1c. Figure 4 presents the distribution matrix of both intra- and inter-SU connections. SU A2 is notable for showing the most connections, linking with all other SUs except for D3a, D1d, and D1e. Generally, inter-SU connections are more frequent between SUs that are stratigraphically close or in lateral continuity. Notably, numerous connections were observed

between A2 and SUs A1, D6, A2R, and D3d base. Despite being few, connections between vertically and horizontally distant SUs also occur, such as between A2 and D1c.

Subsequent spatial and technological analyses were conducted for SUs A2, A1, and D3b alpha. These SUs were selected based on conjoining rates, frequencies of intra- and inter-SU break connections, stratigraphic position, and technological significance. A2 and A1 were chosen for their close stratigraphic relationship, overall high percentages of intra- and inter-SU connections, and their archaeological importance. Although D3b alpha was not identified in the entire eastern half of the cave and contained a relatively low number of blade fragments ($n=70$), it was selected due to its relatively high conjoining rate (18.6%) and the high percentage of intra-SU connections (61.5%). In D3b alpha, we also identified a few additional technological refits (De Stefani, 2003; Falcucci et al., 2020) and excavation documentation shows a dense accumulation of debitage, likely resulting from a single knapping event, near an anthropogenic feature (see SM Fig. S9). Finally, despite their overall high conjoining rates, SUs A2R, D3d, D3d base, and D6 were excluded from further spatial and technological analyses due to their lower percentages of intra-SU connections compared to inter-SU ones.

Spatial Analysis

Figures 5 and 6 illustrate the horizontal distribution of intra- and inter-SU connections, focusing on blade fragments with valid spatial data and consisting of two fragments. Among the studied SUs, A2 is the most extensively excavated and accordingly accounts for most of the intra-SU connections ($n=182$, corresponding to 91 blades), followed by A1 ($n=40$, corresponding to 20 blades). In A2, the distribution of connections is relatively homogeneous, while in A1, connections are concentrated primarily below the cave drip line, with several connections found at the eastern edge of this region (e.g., square 62), where A2 connections are sparse. The rest of the intra-SU conjoining fragments spread quite uniformly in low numbers in the other SUs. In D3b alpha, for instance, the few intra-SU connections are clustered just above the cave drip line.

For inter-SU connections, most fragments are again from A2. The majority of these connections are found between A2 and A1 ($n=31$), followed by D6 ($n=17$), A2R ($n=10$), and D3d base ($n=10$). Beside A2, fragments from A1 connect mostly with D3d base ($n=5$). Notably, A2/A1 connections link regions around the cave drip line with an internal cave region to the east and north of Tunnel C, where A1 is absent. Several connections were also found below the cave drip line (e.g., squares 57, 56, 55, 50). A2R shows a marked interconnection with A2, with several conjoins linking areas where A2R was not identified. The few A2/D3b alpha connections



Fig. 3 Examples of successfully connected blades with their respective conjoining IDs, showcasing the diversity of raw materials. These examples include blades with and without cortical coverage, various levels of thermal alteration, and different degrees of patination. Most blades in this figure consist of two connected fragments, though some examples include three or four fragments. (Photos: A. Falcucci)

($n=3$) link distant areas in the western half of the cave. Finally, connections involving three and four fragments are all inter-SU ($n=11$ and 2, respectively). Six, out of a total of 11 connections made up of three fragments, link A2 with either A1, D3b alpha, D3d, D3d base, or D3a+b sabbie.

Length of Connection Lines

Figure 7a shows the distribution of line lengths for both intra-SU ($n=134$) and inter-SU ($n=110$) connections, categorized by the four classes defined by Cziesla (1990) and the number of connected blade fragments. As expected, the number of intra-SU short lines is significantly higher than that of inter-SU ones (Table 3). Short lines account for 38% ($n=52$) of all intra-SU connections and 6.5% ($n=7$) of all inter-SU connections. Intra-A2 and intra-A1 connections together account for 83% ($n=111$) of all intra-SU connections, not only in the short and medium-distance classes. Most (9 out of 10) of the very long-distance connections come from A2, which also accounts for the majority (20 out of 24) of long-distance connections. Notably, intra-A2 connections include three of the four intra-SU connections made up of three fragments, and one of the two connections made up of four fragments. The frequency of medium- and long-distance lines is quite comparable between intra- and inter-SU connections. Medium-length lines constitute the majority of the inter-SU connections (45.5%, $n=50$), while they account for 36% ($n=48$) of intra-SU connections. Long lines represent 18% ($n=24$) of total intra-SU connections and 22% ($n=24$) of inter-SU connections. Very long lines are significantly more common in inter-SU connections (26%, $n=29$). As expected, shorter connections are more frequent within single SUs (intra-SU). Conversely, longer connections were expected to be more frequent between different SUs (inter-SU). Instead, the frequency distribution of inter-SU shows a peak in the medium range.

Vertical Extension of Connecting Lines

Figure 7b shows the distribution of the absolute vertical distance (ΔZ) between two conjoining fragments, categorized by intra- and inter-SU connections according to Cziesla's classes. As expected, short intra-SU connections cluster around $\Delta Z=0$. Within Cziesla's classes, the distribution of intra-SU connections is right-skewed, with a gradual

increase in ΔZ median values, reaching a median of 0.25 m in the very long class. This median value is comparable to inter-SU very long connections, although the latter display a broader range, with outlier ΔZ values exceeding 0.6 m. Overall, short, medium, and long inter-SU connections exhibit relatively higher ΔZ median values than intra-SU connections, with notable differences between the two categories in the short and medium classes. While higher ΔZ values are expected in inter-SU connections, they still show relatively low values.

Orientation of Connecting Lines

Figure 8 presents the Benn and Rose diagrams for subsets of intra- and inter-SU connections made up of two fragments. It should be noted, however, that only the intra-A2 subset contains a representative number of lines according to Lenoble and Bertran (2004), although the rest of the data still provides interesting insights. The intra-A2 subset ($n=87$) plots at the planar corner of the Benn diagram, suggesting low isotropy overall. The corresponding rose diagram shows a relatively uniform distribution. The subset of long and very long intra-A2 connections ($n=27$) plots closer to the linear corner of the diagram, indicating a less uniform trend in the sample. The intra-A1 sample ($n=20$) shows higher elongation and isotropy indices, with the A1 (long) subset ($n=3$) showing significant directionality toward the E-NE. The inter-A2/A1 sample ($n=27$) plots between the A2 samples, in the planar corner.

Distribution of Thermal Alterations

Figure 9a illustrates the distribution of thermal alterations among blade fragments from the studied SUs. A2 contains the highest number of blade fragments with thermal alterations ($n=27$). Thermal alterations are also found in A1 ($n=2$), D3b alpha ($n=2$), D6 ($n=2$), A2R ($n=1$), and D3d ($n=1$). Figure 9b shows the spatial distribution of thermally altered blade fragments within the intra-A2 subset. Interestingly, burned fragments are found either next to anthropogenic features or adjacent to the eastern wall, to the north of Tunnel C. A very long connection links the latter with feature S17 on the southwestern edge. Similarly, a medium-length line connects a fragment near feature S14 with Tunnel C. Notably, a long line connects a burned fragment with a non-burned one near feature S9. Figure 9c shows the spatial distribution of inter-A2/A1 blade fragment connections with thermal alterations. Two long lines link a region of A2, i.e., the eastern wall to the south of Tunnel C—characterized by a dearth of fragments—with features S9 and S10. Again, a long line connects a burned fragment near feature S9 with a non-burned one.

Table 2 Conjoining rates observed across the analyzed stratigraphic units (SUs), comparing the number of fragments to those successfully connected

SU	Analyzed	Connected	Conjoin. rate (%)	Intra-SU	Inter-SU
D1e	2	0	0.0	0 (-)	0 (-)
D1d	5	0	0.0	0 (-)	0 (-)
D1c	18	1	5.6	0 (-)	1 (100%)
D3a+b	56	4	7.1	0 (-)	4 (100%)
D3a+b sabbie	21	2	9.5	0 (-)	2 (100%)
D3+D6	138	19	13.8	10 (52.6%)	9 (47.4%)
D3a	2	0	0.0	0 (-)	0 (-)
D3b	63	6	9.5	2 (33.3%)	4 (66.7%)
D3b alpha	70	13	18.6	8 (61.5%)	5 (38.5%)
D3d	55	10	18.2	0 (-)	10 (100%)
D3d base	203	36	17.7	16 (44.4%)	20 (55.6%)
D6	231	36	15.6	7 (19.4%)	29 (80.6%)
A1	701	83	11.8	42 (50.6%)	41 (49.4%)
A2R	163	22	13.5	6 (27.3%)	16 (72.7%)
A2	1526	277	18.2	188 (67.9%)	89 (32.1%)
Total	3254	509	15.6	279 (54.8%)	230 (45.2%)

Fragments are classified based on their connections with fragments from either the same (intra) or different (inter) SUs. Percentages are provided in brackets. SUs are generally listed in stratigraphic order, though they may have been identified in different excavation areas (see SM Notes S1 and S2). Rows highlighted in bold indicate the SUs subjected to further analysis in this study. *Conjoin. rate* stands for *Conjoining rate*

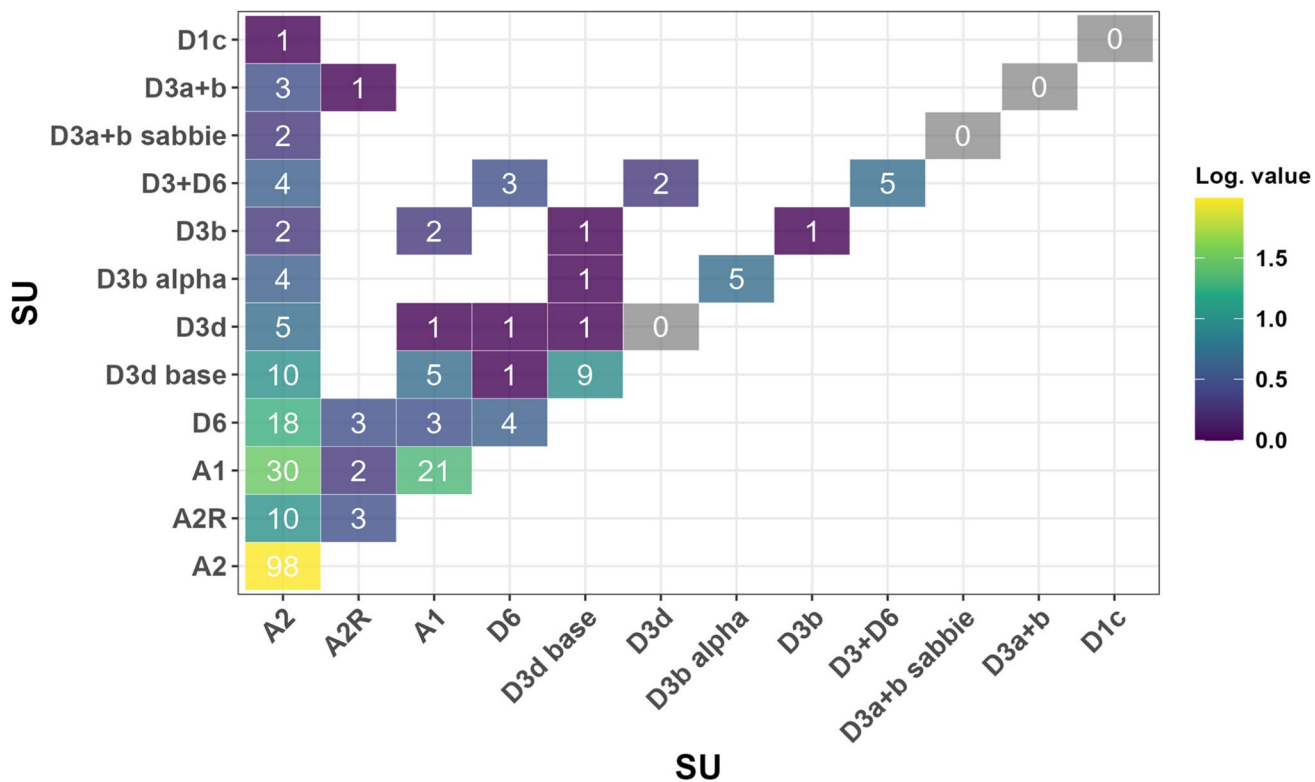


Fig. 4 Distribution matrix of both intra- and inter-SU connections across the stratigraphic sequence at Fumane Cave. The axes indicate SUs in stratigraphic order, though some are not strictly consecutive (see also SM Note S2). The numbers refer to one-to-one connections only; for blanks with three or more fragments, they are divided into pairs. To interpret the figure, start from the lowermost SU A2 along the y-axis and move upwards. Then, read each overlying SU along the x-axis, starting from A2, until reaching the box corresponding to

the intra-SU comparison. From there, move along the y-axis to visualize connections with overlying SUs. The heatmap was generated by log-transforming the total number of connections. Darker colors indicate a low number of connections, while lighter colors signify a higher number. Zero values (in gray) are included only for the same-SU intersection to complete the diagonal but not in other comparisons to enhance readability. SUs with no identified connections (D1e, D1d, D3a) are excluded from the figure

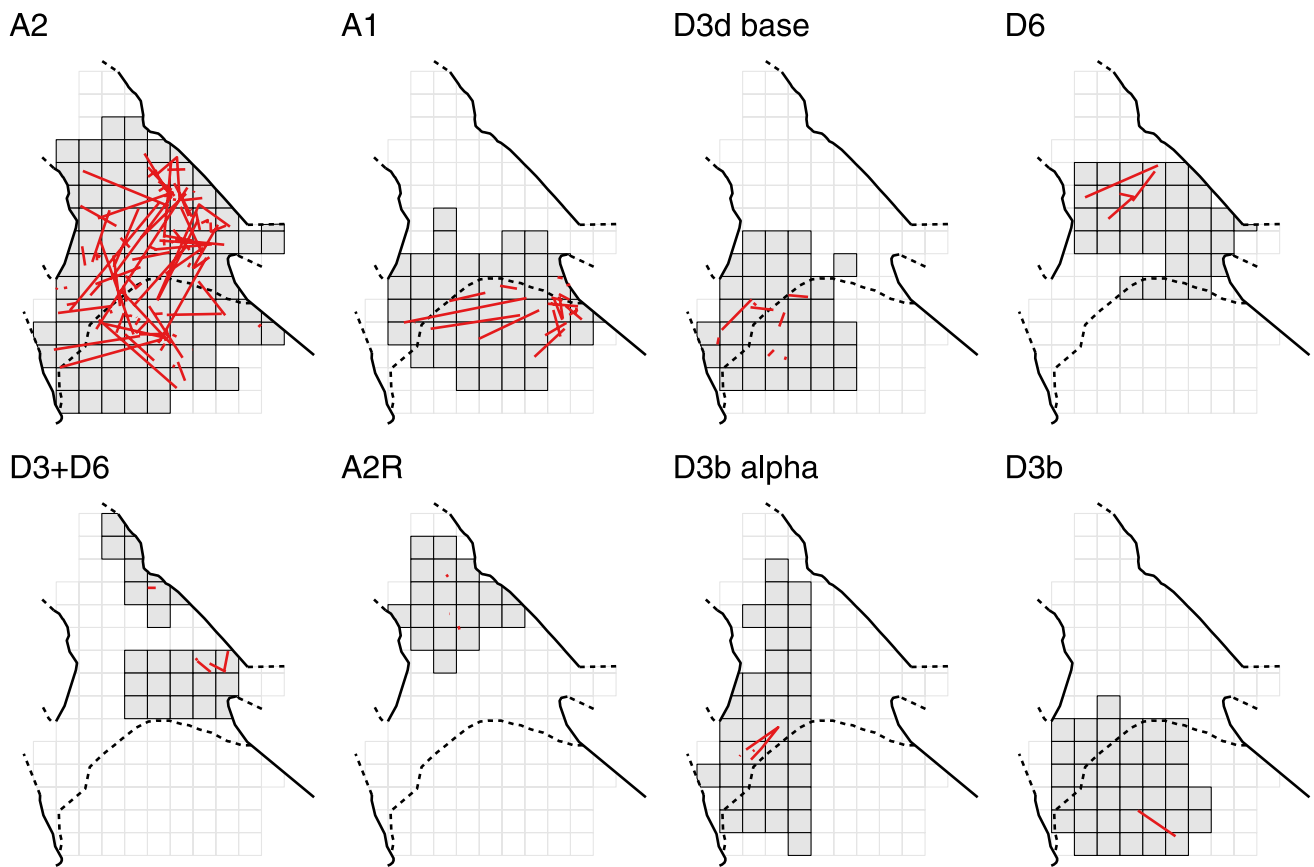


Fig. 5 Spatial distribution of intra-SU connecting blade fragments. Filled gray squares represent excavated squares of the different SUs. A very light gray is used in the background to mark the entire grid

Standardized Fracture Ratio (SFR)

Figure 10 displays the areal distribution of two subsets of observed cases (O) of blade fragments in A2: (a) the whole sample, and (b) the subset of short and medium connections. It also shows the expected cases (E) of complete blades and the SFR of O/E. Interestingly, in both cases, a dense cluster of blade fragments is observed along the eastern wall of the cave, just to the north of Tunnel C, with the highest count in square 110. It is worth noting that the same square also shows a high number of complete blades. Similar densities between observed and expected cases are seen in squares 55, 56, 65, and 66, just outside the cave drip line, where low SFRs are observed. On the other hand, squares 77 and 95 stand out due to their very high SFRs, indicating a significantly higher number of blade fragments than complete blades. Remarkably, the features S16 and S14 are found in squares 77 and 95, respectively. Nevertheless, anthropogenic features are also present in squares with low SFR values, such as S10.

Figure 11 shows the areal distribution of intra-A2 blade fragment connections by Cziesla (1990) length classes. Two regions of the cave are marked by relatively high fragment

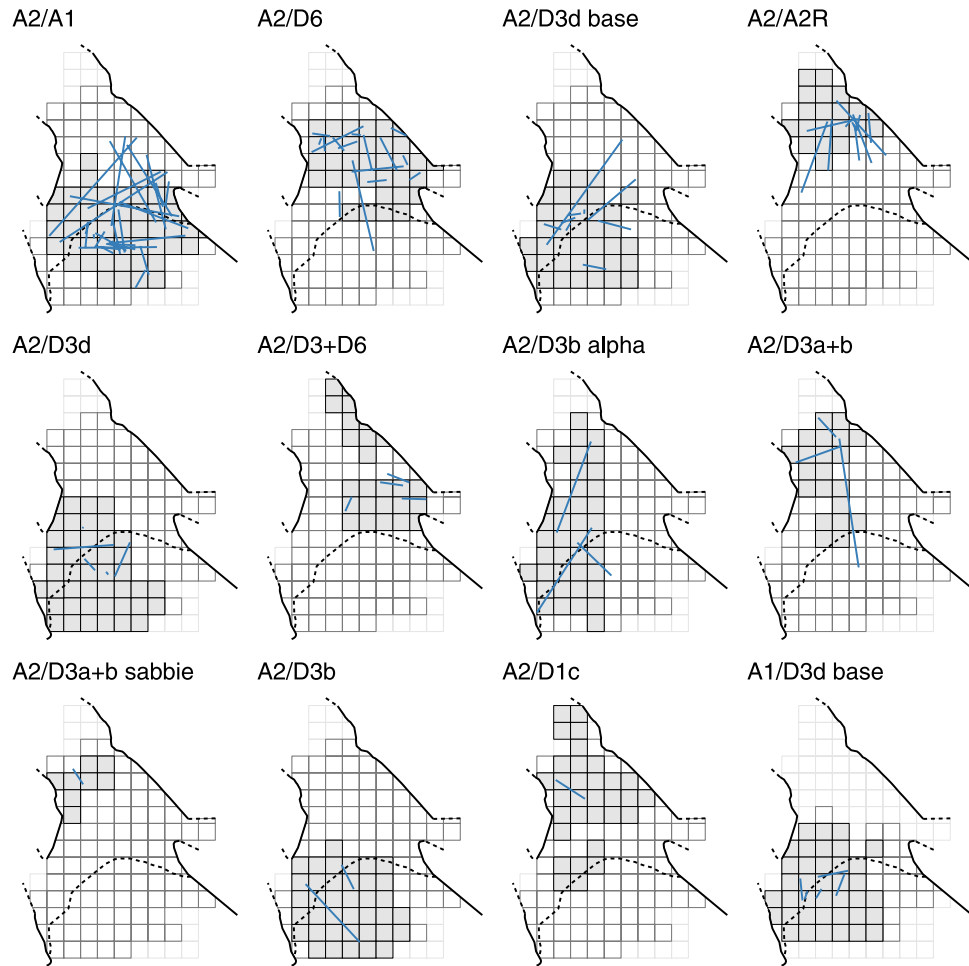
densities across all distance classes: the eastern wall to the north of Tunnel C and the area just below the drip line. Moreover, the intra-A2 very long connections include more fragments in the same squares where short connections are mostly found. Thus, connection length cannot be used in this specific case as a factor to assess the integrity of the SU.

Discussion: Part One

Framing the Results of the Break Connection Program

Fumane Cave contains one of the most important archaeological deposits of the late Pleistocene, spanning Middle to Upper Paleolithic technological complexes from MIS 4 to the onset of Heinrich Event 3 (Peresani, 2022). The wealth of evidence collected over the last decades of excavations has enabled archaeologists to explore several intensely debated biocultural processes, such as the demise of Neanderthals and the spread of *Homo sapiens* across Europe. In particular, the Uluzzian from SU A3 and the Protoaurignacian from

Fig. 6 Spatial distribution of inter-SU connections between A2 and other SUs, as well as between A1 and D3d base. Filled gray squares represent excavated squares of A2 (and A1 in the bottom right plot). Lighter gray empty squares indicate the excavated squares of the connected SUs. In the background, a very light gray is used to mark the whole grid



SUs A2 and A1 represent pivotal points for discussions about the onset of the European Upper Paleolithic.

However, modeling high-resolution population dynamics and chrono-cultural processes from field-defined stratigraphic SUs requires a thorough examination and assessment of the integrity and reliability of the archaeological deposit and analytical units, especially at a site characterized by complex formation processes and a long history of excavations, during which different excavation protocols were employed. This study addresses this significant research gap by employing a highly efficient lithic taphonomic analysis, specifically the lithic break connections method (Bordes, 2000), combined with a comprehensive spatial analysis of blade fragment connections. Based on the results of these primary taphonomic analyses, we will conduct a renewed technological analysis of selected regions within key SUs and compare our findings to previous analyses conducted at the site.

Regarding the lithic break connection program, the first point to emphasize is the overall high conjoining rate we achieved (15.6%). This is a significant accomplishment, particularly given the challenges posed by the frequent

patination of blade fragments made from the Maiolica raw material, which is more prone to patination (Bertola, 2001). This characteristic significantly complicated and slowed down the systematic trials for connections. When we examine the success rates and the available relevant information from other published break connection studies (Table 4), Fumane stands out as the site with the highest conjoining rate, followed by Le Piage (14.8%; Bordes, 2002) and Warwas (14.5%; Tsanova, 2013).

It is reasonable to assume some degree of correlation between the extent of the excavation area and the number of connections typically identified (Bordes, 2000). Nevertheless, Warwas, a small-sized excavation, yielded a relatively high rate of connections. Similarly, sample size might play a critical role, as a larger sample is expected to increase the success rate, while also slowing down the systematic search for break connections. However, this is not always the case, as other factors are likely at play. For instance, Gravina et al. (2018) considered a large lithic assemblage but reported poor results. While the authors appropriately discussed site preservation issues, an aspect that was less considered involves the selection of flakes instead of blades. Flakes are

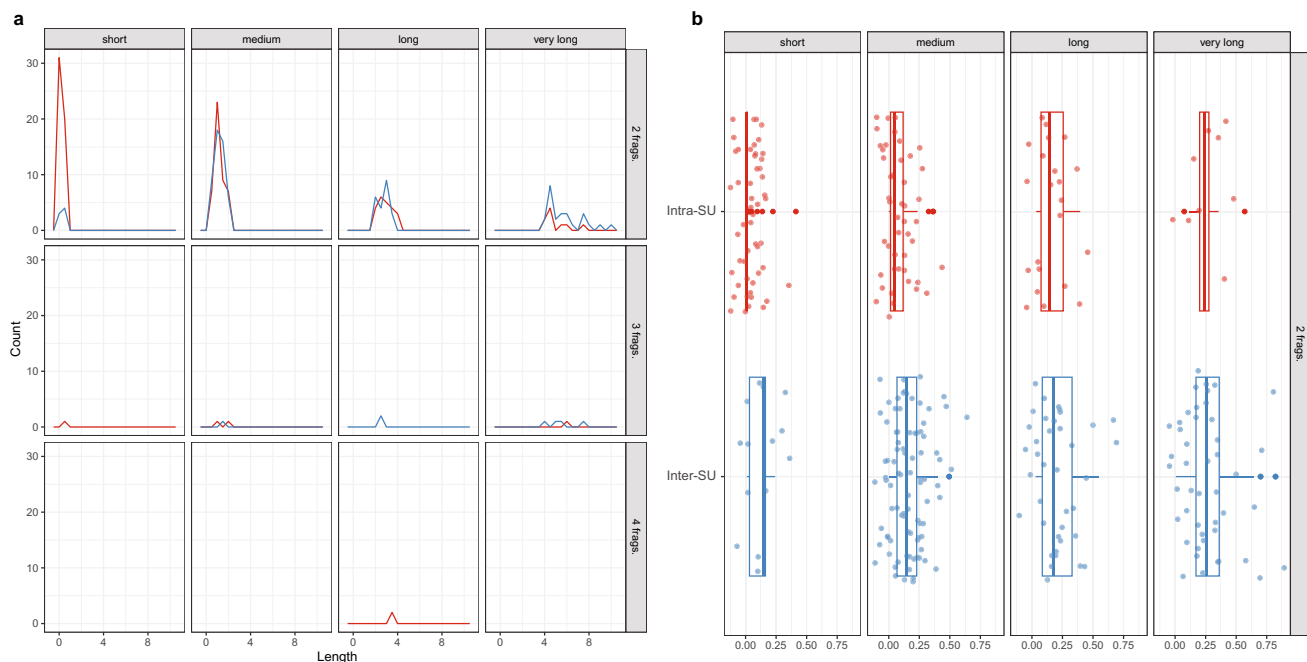


Fig. 7 **a** Length distribution of intra- (red) and inter-SU (blue) connecting lines by the number of connected fragments (two, three, and four) and Cziesla's length classes; **b** Absolute vertical distances

between two connecting blade fragments, categorized by Cziesla's length classes and type of connection: intra- (red) and inter-SU (blue)

Table 3 Frequency of intra- and inter-SU connections, divided according to the distance classes by Cziesla (1990)

Cziesla's class	Intra-SU (%)	Inter-SU (%)
Short	38	6.5
Medium	36	45.5
Long	18	22
Very long	8	26

less standardized in terms of morphology, which we argue drastically reduces the number of identifiable connections.

Thus, the high conjoining rate obtained at Fumane supports our initial assumption that at least some SUs and areas of the archaeological excavation are well-preserved. SUs such as A2, A2R, A1, D6, D3d base, D3d, D3b alpha, and D3 + D6 all have conjoining rates higher than 10%, while other SUs exhibit quite low conjoining rates (see Table 2). For the non-conjoined fragments (84.4%), several factors may contribute to the lack of connections. Besides the aforementioned natural and anthropogenic processes, other factors could include analyst errors, surface alterations, and high fracture rates, all of which reduce the success of connection attempts. As shown in Table 4, however, Fumane stands out due to the high number of inter-SU connections identified ($n=116$), which account for approximately 44% of the cases. This suggests that the numerous SUs documented during the archaeological excavations do not represent true

stratigraphic divisions in the geological sense. Notably, when SUs A2, A2R, and A1 are considered as a single analytical unit based on the spatial analysis results (see the “Identifying the Best-Preserved Areas of the Excavation for Renewed Chrono-Cultural Studies” section), the intra-SU connections increase to approximately 72% ($n=188$), aligning with the range observed at the other sites compared.

A2 stands out among the other SUs with the highest number of analyzed ($n=1526$) and connected ($n=277$) fragments, one of the highest conjoining rates (18.2%), and the highest percentage of intra-SU connections (67.9%). It also serves as the reference SU for the study of most of the inter-SU connections. A2 likely represents a period of more intense and frequent use of the cave, possibly due to multiple short-term occupational events (Marcazzan et al., 2022). A thorough investigation of A2 is therefore fundamental. After A2, A1 yielded the highest number of connected fragments ($n=83$), nearly equally split between intra- (50.6%) and inter-SUs (49.4%).

Regarding inter-SU connections, A1 is also the SU most closely linked to A2. While A2R, D6, D3d base, D3d, D3b alpha, and D3 + D6 exhibit higher conjoining rates than A1, the overall number of connections is much lower. After A2 and A1, D6 and D3d base yielded the highest number of connections (33 and 28, respectively) and significant conjoining rates (15.6% and 17.7%, respectively). However, these SUs have the highest numbers of inter-SU connections with A2. A similar pattern is observed for A2R, where the number of

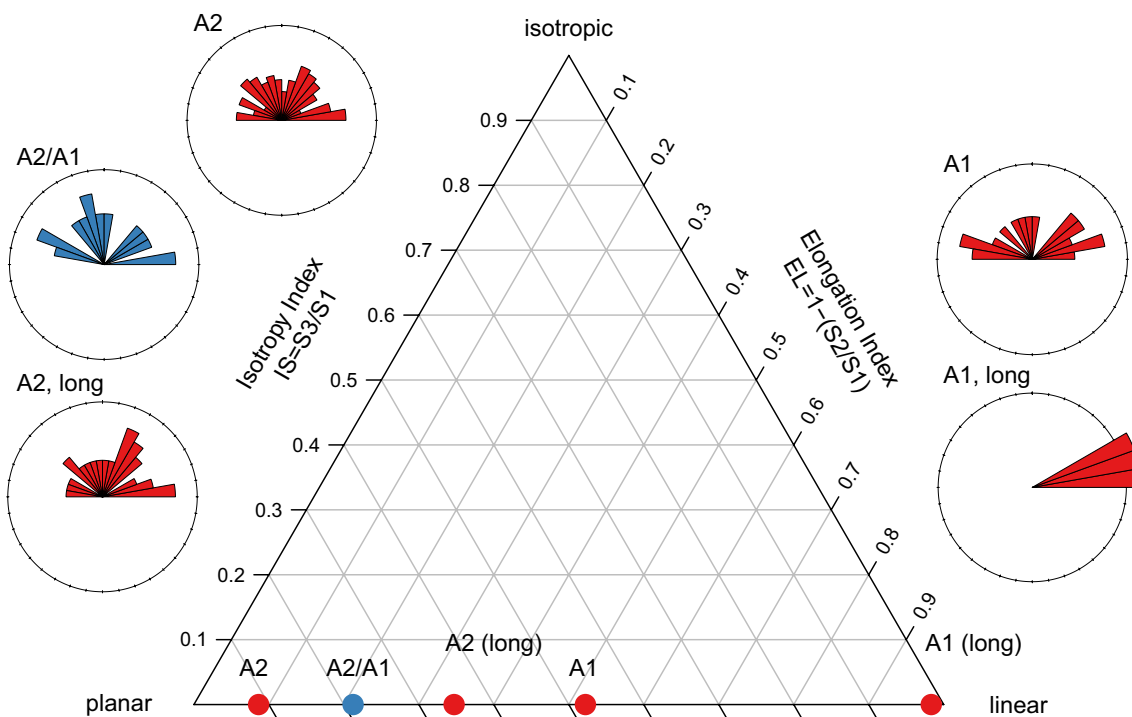


Fig. 8 Benn diagram showing the orientation patterns of intra- (red) and inter-SU (blue) connections. Rose diagrams show the bearings of connecting lines. Subsets of long and very long intra-A2 and intra-A1 connecting lines are also shown

connections with A2 is three times greater than the intra-SU connections identified. The predominance of inter-SU over intra-SU connections in these SUs led us to exclude their lithic assemblages from further technological analysis.

On the other hand, D3b alpha is the only SU from the D sedimentary complex that yielded a high percentage of intra-SU connections (61.5%), along with additional technological refits, evidence of an anthropogenic feature, and on-site knapping, albeit partly rearranged by post-depositional processes (De Stefani, 2003; Falcucci et al., 2020; Peretto et al., 2004). These observations, coupled with the low thickness of the SU and its increased organic content, suggest its cultural content is worth investigating further to understand the development of the Aurignacian at the site, despite the low number of lithics recovered and its identification only in the western portion of the cave.

Recent studies on the micro- and macro-fauna have highlighted that the D3 complex accumulated during Heinrich Event 4 (López-García et al., 2015; Marín-Arroyo et al., 2023), underscoring its archaeological importance in the debate surrounding the transition from the Protoaurignacian to the Early Aurignacian (Banks et al., 2013a). It is important to note that the previous technological study merged the D3b alpha assemblage with that from D3d (Falcucci et al., 2020). However, D3d contains only inter-SU connections and none with D3b alpha. Additionally, a recently dated bone with cut marks from D3d (Marín-Arroyo et al., 2023)

has a 14C age of $36,100 \pm 1400$ years (OxA-41260), which is very close to the dates obtained from the underlying A2 and A1 SUs and about 2000 years younger than the 14C age from D3b alpha (Higham et al., 2009). We are thus prompted to reject this past stratigraphic correlation.

To summarize, these results led us to focus exclusively on A2, A1, and D3b alpha for further spatial analyses. These analyses enabled us to identify specific areas within these SUs, based on their relatively good preservation, for conducting new technological assessments.

Identifying the Best-Preserved Areas of the Excavation for Renewed Chrono-Cultural Studies

A2 is the most extensively excavated SU at Fumane, while A1 was excavated primarily in the cave exterior and near the drip line. In contrast, D3b alpha is confined to the western half of the cave (see SM Note S2). Interestingly, A1 yielded a relatively high number of connections compared to other SUs with similar areal coverage. When considering the spatial distribution of intra-SU connections within A2 and A1, as well as inter-SU connections between A2 and A1, a clear pattern of interrelation emerges. Intra-A1 short and medium connections are concentrated in a region with a low density of intra-A2 connections, specifically in squares 52, 53, 62, 63, 72, and 73 to the southeast (see Fig. 5). Moreover, this particular region is

linked by inter-A2/A1 connections to other areas characterized by high densities of material in A2 (see Fig. 6), such as the northeastern wall adjacent to Tunnel C (e.g., squares 115, 91, and 92) and a small central area of the cave below the drip line around feature S10 (e.g., squares 55, 56, 65, and 66).

Directional patterns are evident in both A2 and A1, as well as in the connections between them, with E-W very long connections outside the cave and SW-NE very long connections inside the cave being common (Figs. 6 and 7a). These directional patterns are clearly illustrated in the Benn and Rose diagrams (see Fig. 8). All our samples exhibit a low degree of isotropy, indicating a minimal impact of chaotic processes typically associated with large-scale slope movements, such as creep, solifluction, mudslides, debris flows, and dry grain flows (Lenoble & Bertran, 2004). However, a certain degree of linearity is observed in the preferential orientation of subsets of material, particularly in the long-distance connections within A1. While strong linearity could be associated with massive processes like solifluction or mudslides (Discamps et al., 2023), anisotropic patterns may also result from anthropogenic activities. For example, trampling has been linked to clear orientation patterns in both cave and open-air sites, as well as in experimental settings (Benito-Calvo et al., 2011; Driscoll et al., 2016; Eren et al., 2010; Martini et al., 2021; Marwick et al., 2017; McBrearty et al., 1998; Miller et al., 2010; Weitzel & Sánchez, 2021). The inter-SU connections between A2 and A1 exhibit a pattern that lies between the A2 and A1 samples on the Benn diagram, trending towards the planar corner (Fig. 8). This pattern closely resembles that of the long A2 connections, which several studies have associated with undisturbed lithic assemblages (Discamps et al., 2023, among others).

Despite the relatively frequent long and very long connections typically associated with heavily reworked sequences, the high rates of short and medium connections occurring in the same areas, along with the overall spatial pattern of intra-A2, intra-A1, and inter-A2/A1 connections, suggest minimal reworking by post-depositional processes. A cluster of medium and long A2/A1 connections is again observed just outside the cave (squares 55–75, 56–76; Fig. 12), a region also highlighted in Fig. 11 for its high density of short connections in A2. Notably, several burned fragments were found in A2 around feature S10 in square 55, some of which connect with A1 in the same area or form long connections with a burned fragment in square 63, thus again linking the southeast with the area around S10 (see Fig. 9).

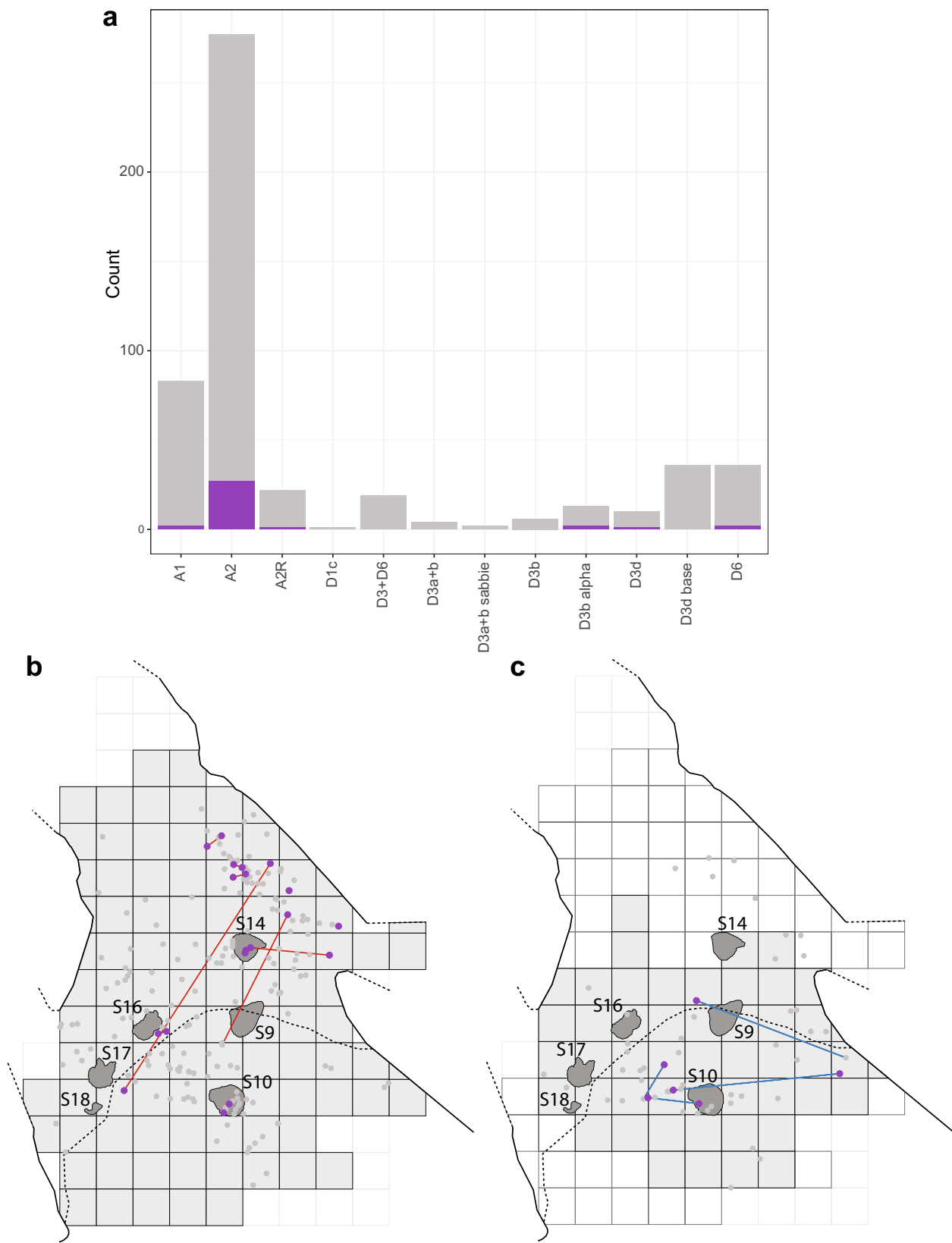
The significant degree of interrelation between A2 and A1 is further indicated by the relatively short absolute vertical distances (ΔZ) among conjoined fragments. Most A2/A1 connections fall within the medium and very long Cziesla's categories. While the ranges of vertical distances in these length categories are broader than those observed in intra-SU connections, the median values remain relatively low,

around 0.10 m and 0.25 m, respectively (Fig. 7b). These values suggest limited vertical dispersion of material, even across SUs. Interestingly, similar vertical displacement values have been recorded and attributed to burrowing activities, as rodent burrows can cause vertical displacements of up to 30 cm (Bocek, 1986, 1992).

The combined evidence suggests that A2 and A1 should be interpreted as two facies of the same SU. This interpretation is well supported by the results of the spatial analysis, which indicates minimal influence from post-depositional processes in the displacement of broken blades. To further substantiate these findings through a quantitative comparison of the cultural content in the two SUs, we identified three areas of the excavation deemed suitable for renewed techno-typological investigations (SM Fig. S15a). These areas were selected primarily based on the short- to medium-length connection conjoining rates and the overall sample of blade fragments (see Fig. 10b), which highlight these regions for their high conjoining rates. Interestingly, some of these square meters were also sampled by Falcucci et al. (2017) due to their high lithic densities.

The first area (A2int, internal) is located in the northeastern sector of the cave, encompassing seven square meters (i.e., squares 95, 100, 105, 110, 115, 120, 125). This area is also characterized by a cluster of burned fragments (see Fig. 9b) and several long connections. Notably, the sediments in this sector are compressed towards the eastern cave wall, suggesting that post-depositional processes may have influenced the movement of lithics towards the cave interior. However, considering the connection patterns (Figs. 10b–11) and the distribution of thermal alterations (Fig. 9b), other factors likely played a role as well. For example, lithics discarded during different occupation events may have been routinely removed from the main dwelling area to clean the living floor (Bel et al., 2020). Trampling by both humans and animals might have also contributed (Marwick et al., 2017), along with differential use of space (Romagnoli & Vaquero, 2019).

The second area (A2ext, external) includes and surrounds the feature S10, covering square meters 55, 56, 65, and 66. For spatial consistency, all lithics from A1 in squares 55, 56, 65, and 66 were also sampled, designated as the A1ext assemblage. We excluded square meters near feature S16 (e.g., square 77) from these selections because these regions, as per the SFR analysis, showed a higher frequency of broken blades compared to complete blades, making them less suitable for technological studies. It is noteworthy that this feature contains charcoal dated to $34,180 \pm 270$ BP (OxA-19414), which is considerably younger than other charcoals from A2 (Higham et al., 2009), potentially indicating post-depositional processes or stratigraphic issues in this area, as also noted by Banks et al. (2013b). Interestingly, Marcazzan et al. (2022) defined S16 as an occupation horizon characterized by several short and repeated occupations, rather than a hearth.



◀Fig. 9 **a** Frequency distribution of thermal alterations (purple) recorded in our sample of connecting blade fragments; **b** Spatial distribution of thermal alterations (purple dots) in the intra-A2 subset of connecting blade fragments. Filled gray squares represent excavated squares of A2. Gray dots indicate fragments with no thermal alterations; **c** Spatial distribution of thermal alterations (purple dots) in the inter-A2/A1 subset of connecting blade fragments. Filled gray squares represent excavated squares of A1. Light gray empty squares indicate excavated squares of A2. The features are drawn and labeled with “S” and their respective numbers. A recent study has provided additional information for S16, S17, and S18. S17 is identified as a “hearth with a change in clay color”, while S18 and S16 are classified as occupation horizons (Marcazzan et al., 2022)

The third area is in the southeastern portion of the excavation (squares 62, 63, 72, and 73), where only material from A1 will be analyzed (A1east). This selection is based on the high number of intra-A1 connections and the high density of lithics in this region. This sampling strategy will allow us to explore the techno-typological variation between A2 and A1 across the excavated area. We anticipate finding a significant degree of technological similarity between the sampled subsets on both inter- and intra-SU levels. Selecting different areas will also enable us to address the intra-site spatial variability, providing new data to initiate discussions surrounding possible differences in the activities conducted at Fumane during the formation of the Protoaurignacian sedimentary body.

Due to the limited sample size, we were unable to identify any area in D3b alpha suitable for technological analyses through the break connection program and spatial analyses. Nevertheless, we selected D3b alpha based on other archaeological evidence (e.g., limited thickness, presence of an anthropogenic feature, evidence of on-site knapping, and additional technological refits, as previously described). It is important to reiterate that the D3b alpha dataset differs from the one published by Falcucci et al. (2020) because this SU was previously correlated with D3d. We sampled D3b alpha across all square meters up to the line of squares in the 80 s (SM Fig. S15b). We excluded the thin SU, also named D3b alpha, from the innermost area of the cave, as this correlation could not be confirmed by either fieldwork evidence or our break connection study. Although the selection of D3b alpha is not fully supported by our spatial analysis, it is crucial for testing the hypothesis of cultural continuity of the Protoaurignacian in northeastern Italy.

Results: Part Two

Overview of the Lithic Assemblages and Intra-Site Variation

Table 5 presents the frequencies of lithic artifacts in the sampled subsets, revealing that both A2 subsets yielded more lithics than the others. Notably, A2int stands out with the highest number of lithics, consistent with the density

of materials found in the northeastern area of the cave. The variation in the distribution of different lithic classes among the assemblages is significant, with a higher proportion of cores observed in A1east and D3b alpha, and a lower proportion of retouched tools in A2int. An examination of the typological list (Table 6) shows that retouched bladelets, which are characteristic of the Protoaurignacian at Fumane, are less common in A2int compared to A2ext, A1ext, and A1east. On the other hand, tools such as end-scrapers and retouched flakes are more frequent in A2int. Variability is also evident in the distribution of blank types, as shown in SM Fig. S16. A2int contains fewer bladelets and a higher frequency of flakes.

Core reduction, encompassing the initialization phases to the production of desired blanks, was conducted in both areas of the cave. This is corroborated by the distribution of flakes, blades, and bladelets categorized according to different phases of core reduction (refer to SM Figs. S17–19), as well as the presence of cortex on blanks and tools (Table 7). Both initialization and maintenance blanks are evenly distributed among the A2int, A2ext, A1ext, and A1east assemblages. D3b alpha, however, is characterized by a slightly higher proportion of initialization blanks. The higher frequency of initial cores (Table 8) in both A2int and A1east somewhat contrasts with these observations, possibly suggesting that the initial phases of core shaping were more frequently conducted in these areas.

Technological Variability between and within Stratigraphic Units

All lithic subsets are characterized by a high proportion of laminar blanks, particularly bladelets. The only exception is D3b alpha, where flakes are present in equal proportions to laminar blanks (see SM Fig. S16). SM Figure S20 shows that all subsets exhibit a linear distribution in the size of blades and bladelets, a pattern commonly associated with the production of both blades and bladelets from the same cores (Tsanova, 2008). Interestingly, we observed notable differences in the sizes of the produced blades and bladelets. Blades from the external areas of the cave in A1 and A2 are slightly narrower and thinner, though not shorter, compared to their counterparts in the internal (A2int) and eastern (A1east) areas (see SM Figs. S21–S23). Moreover, the morphological and technological features of the blades do not vary significantly across the assemblages. Scar patterns on blades are predominantly unidirectional and subparallel (see SM Table S1). Similarly, no significant differences were identified in attributes such as blade twisting and curvature in profile view, cross-section shape, and external morphology (see SM Tables S2–S5). This

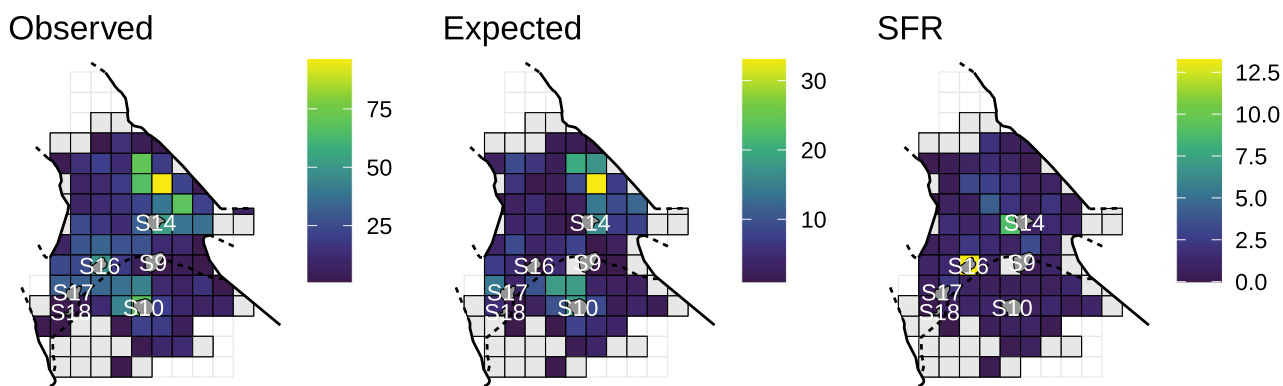
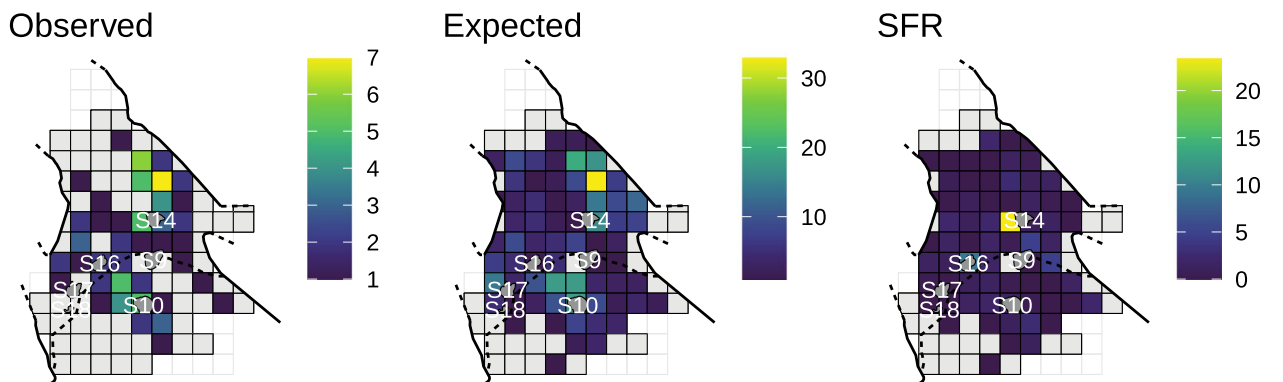
a**b**

Fig. 10 **a** Areal distribution of observed blade fragments in A2 (O); areal distribution of expected complete blades in A2 (E); Standardized Fracture Ratio (SFR) of O/E in A2; **b** Areal distribution of observed short and medium blade fragment connections in A2 (O);

areal distribution of expected complete blades in A2 (E); SFR of O/E in A2. Filled gray squares represent excavated squares of A2 devoid of finds. A very light gray is used in the background to mark the entire excavation grid

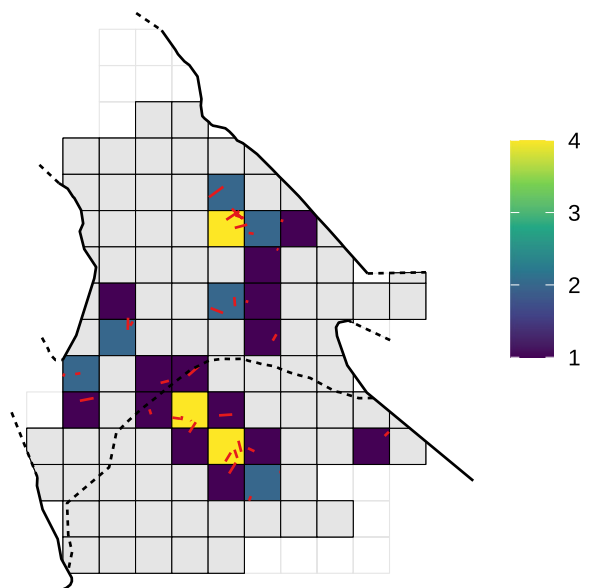
uniformity also extends to the platforms of the blanks, which are mostly plain (see SM Table S6).

More pronounced differences were observed in the bladelet assemblages compared to the previous study by Falcucci et al. (2020). Bladelets from D3b alpha are significantly smaller in all linear dimensions (SM Figs. S24–S26) and are also less elongated (SM Fig. S27). Conversely, bladelets from A1east are longer and wider compared to most of the assemblages. Although a similar pattern within A1 was partially noted by Falcucci et al. (2020), it is now evident that this size variation is specific to the eastern area of A1. Importantly, this variability is not related to the use of different raw material types, as Maiolica remains the predominant raw material, and the longer bladelets are consistently made from this variety (SM Fig. S28).

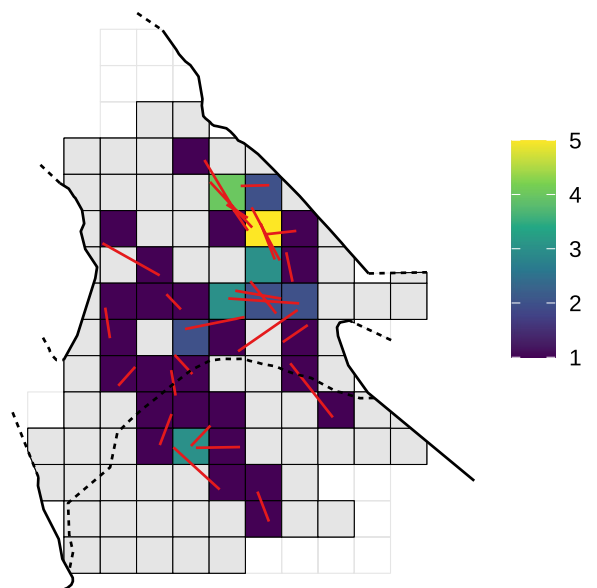
The morphological and technological attributes recorded on bladelets exhibit minimal variability across the studied assemblages (SM Tables S7–S12). To better interpret these results and take advantage of the larger number of

available complete bladelets, we conducted further investigation using MCA, focusing only on non-modified complete bladelets. Seven categories were considered: elongation, robustness, profile curvature, profile twisting, scar pattern organization, outline morphology, and distal end morphology. The first two dimensions of the MCA explain approximately 38% of the total variance (SM Fig. S29). Attributes related to the degree of convergence in outline morphologies and distal ends, as well as scar pattern direction, significantly contribute to the construction of the first two dimensions. This is also true for bladelets with low robustness and high elongation values (SM Fig. S30). The scatterplot in Fig. 13a illustrates that these attributes contribute more to the first dimension of the MCA. The resulting ANOVA tests confirm that most of the variability is described by the first dimension (Fig. 13b), with bladelets from A1east being the most distinct among the studied assemblages. In contrast, bladelets from D3b alpha are not significantly different from those in A1ext and A2ext.

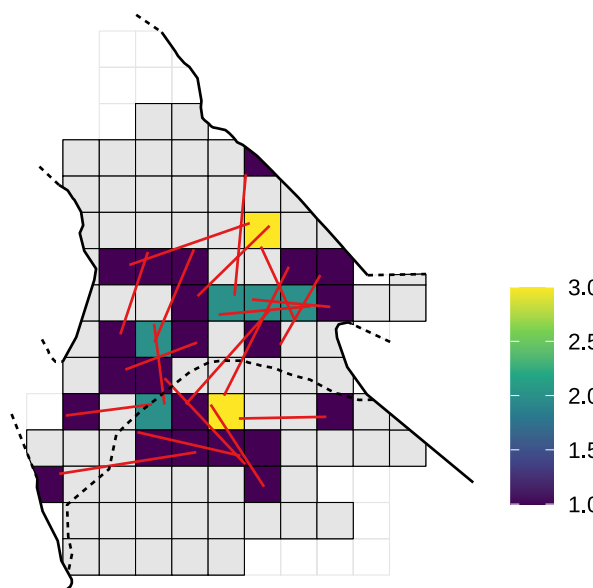
Short



Medium



Long



Very long

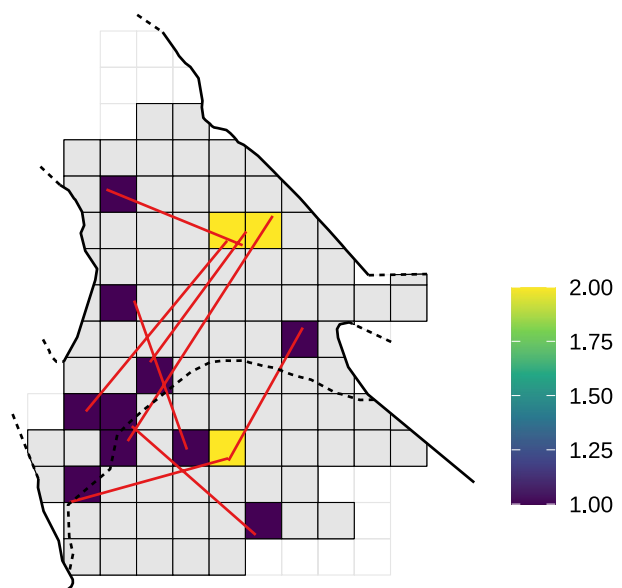


Fig. 11 Areal distribution of intra-A2 connecting fragments by Cziesla's classes (i.e., short, medium, long, and very long). The total number of connecting fragments in each square is color-scaled, with yellow squares indicating higher fragment densities and blue squares

indicating lower densities. Filled gray squares show excavated squares of A2 devoid of finds. In the background, a very light gray is used to mark the whole excavation grid

Attributes recorded on the bladelets' platforms suggest a possible shift in knapping techniques from A2–A1 to D3b alpha. The presence of less developed lips and a higher number of moderately formed bulbs might indicate the use of a different type of hammerstone or a change in knapping gesture. Additionally, there are more linear and punctiform

platforms in D3b alpha, although the differences compared to the other assemblages are not statistically significant (SM Tables S13–S15). However, caution is needed in interpreting this aspect, as variability between individual knappers is likely to be a significant confounding factor (e.g., Driscoll and García-Rojas, 2014; Roussel et al., 2009).

Table 4 Comparison of Fumane's results with data from other studies that have employed the break connection method to assess assemblage integrity and site formation processes

Site	Technocomplex	Site type	m ²	Layers	Sample size	Conn. frag	Nr. conn	Intra vs. inter	Success rate	Reference
Basté	Châtelperronian	Open air	17	4	390	32	16	13–3	8.2%	(Bachellerie, 2011)
	Aurignacian	Rockshelter	37	3	1117	104	52	42–10	9.3%	(Bordes, 2000)
Cova de les Cendres	Solutrean, Gravettian, Aurignacian	Cave	12–3	6	1236	60	31	24–7	4.8%	(Bel et al., 2020)
	Gravettian, Aurignacian	Cave	107	15	3,254	509	262	146–116	15.6%	This study
Grotte XVI	Aurignacian, Châtelperronian	Cave	-	3	-	-	14	12–2	-	(Lucas et al., 2003)
Le Piage	Aurignacian, Châtelperronian	Cave	84	5	229	34	17	13–4	14.8%	(Bordes, 2002)
Roc-de-Combe	Aurignacian, Châtelperronian	Rockshelter	6	2	452	14	7	7–0	3.1%	(Bordes, 2002)
Saint Césaire	Châtelperronian, Mousterian	Rockshelter	32	3	1441	58	29	21–8	4%	(Gravina et al., 2018)
Tennata IV	Initial Upper Paleolithic	Cave	25	3 phases	824	87	51	44–7	10.6%	(Tsanova, 2008)
Warwasi	Baradostian, Mousterian	Rockshelter	8	3	426	62	31	30–1	14.5%	(Tsanova, 2013)

Conn. Frag., stands for connected fragments; *Nr. Conn.*, stands for the number of connections. The *Intra vs. inter* column reports the total number of connections identified within and across archaeological layers.

Except for the Saint-Césaire analysis, all studies attempted to connect laminar fragments and laminar flakes. Additional notes for some sites are as follows: (1) At Caminade, other connections were identified in the *Bergeracois* chert, but the numbers are mixed with other technological refits, making it difficult to ascertain the exact number of conjoined blades; (2) At Cova de les Cendres, the excavated area decreased (to as small as 3 m²) as archaeologists progressed deeper into the stratigraphic sequence; (3) At Le Piage, more conjoins were found in the chert types *Sénionien noir* (*n* = 576) and other rare raw materials (*n* = 245). However, blade fragment data are not separated from other technological refits. Additionally, the conjoining activity on *Sénionien noir* considered only one layer; (4) At Tennata, 15 debitage connections were removed for consistency in comparison. In the intra- and inter-layer quantification, these pieces (making up six blanks) were not excluded from the count because it was not possible to determine which category they belonged to; (5) At Warwasi, the conjoining rate is considered differently in this table, as the author used the number of connected pieces instead of the total number of connected fragments (see Table 2 in Tsanova, 2013).

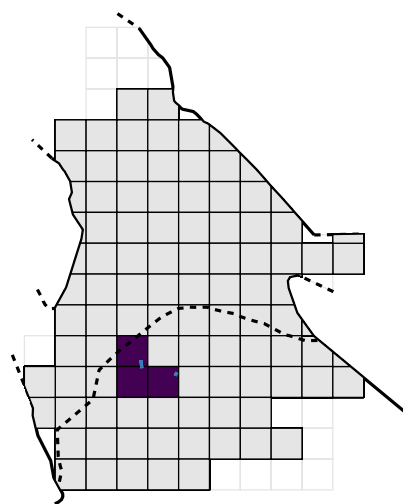
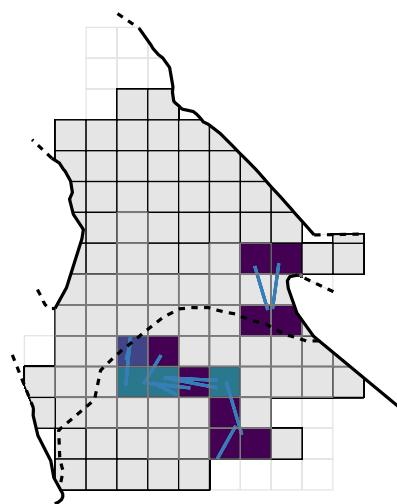
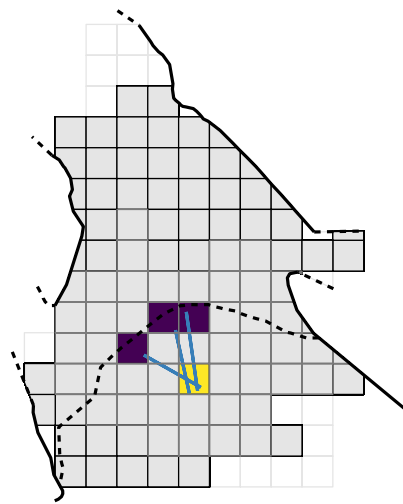
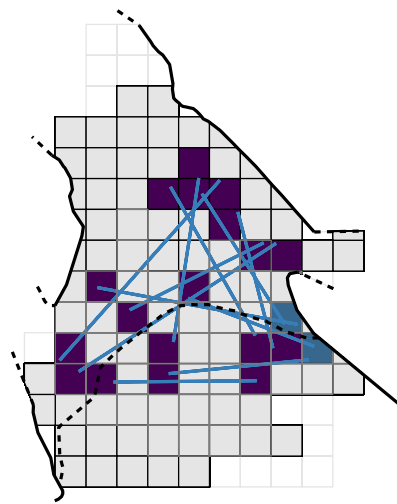
Short**Medium****Long****Very long**

Fig. 12 Areal distribution of inter-A2/A1 connecting fragments by Cziesla (1990) classes (i.e., short, medium, long, and very long). The total number of connecting fragments in each square is color-scaled,

with yellow-colored squares indicating higher densities of fragments, and blue-colored squares indicating lower densities. Light gray empty squares show excavated squares of A2

Table 5 Quantification of the assemblages based on the main lithic classes

Class	A2int	A2ext	A1ext	A1east	D3b alpha
Angular debris	236 (5.7%)	204 (8.5%)	28 (3.7%)	59 (6.1%)	19 (4.8%)
Blank	3557 (86.3%)	1911 (80.0%)	599 (80.1%)	735 (75.8%)	313 (79.0%)
Core	25 (0.6%)	12 (0.5%)	2 (0.3%)	22 (2.3%)	10 (2.5%)
Tool	303 (7.4%)	263 (11.0%)	119 (15.9%)	154 (15.9%)	54 (13.6%)
Total	4121	2390	748	970	396

Lithics classified as both cores and tools (e.g., carinated endscrapers) are included in the core list only. Artifacts below 1.5 cm in maximal dimensions are excluded from this table. Percentages are presented in brackets

Table 6 General overview of the main tool categories recovered across the studied areas, with percentages reported in brackets

Typology	A2int	A2ext	A1ext	A1east	D3b alpha
Blade Aurignacian	0 (-)	0 (-)	0 (-)	1 (0.6%)	0 (-)
Blade pointed	3 (1.0%)	0 (-)	0 (-)	0 (-)	0 (-)
Blade retouched	41 (13.4%)	20 (7.6%)	7 (5.8%)	9 (5.8%)	3 (5.2%)
Bladelet retouched	175 (57.4%)	219 (83.0%)	103 (85.8%)	133 (85.3%)	34 (58.6%)
Burin multiple	2 (0.7%)	1 (0.4%)	2 (1.7%)	1 (0.6%)	0 (-)
Burin simple	12 (3.9%)	10 (3.8%)	4 (3.3%)	0 (-)	2 (3.4%)
Composite tool	9 (3.0%)	4 (1.5%)	1 (0.8%)	1 (0.6%)	0 (-)
Endscraper carinated	1 (0.3%)	0 (-)	0 (-)	0 (-)	3 (5.2%)
Endscraper simple	21 (6.9%)	2 (0.8%)	3 (2.5%)	4 (2.6%)	3 (5.2%)
Endscraper thick-nosed	0 (-)	0 (-)	0 (-)	0 (-)	1 (1.7%)
Flake retouched	24 (7.9%)	2 (0.8%)	0 (-)	5 (3.2%)	5 (8.6%)
Rabot	1 (0.3%)	1 (0.4%)	0 (-)	1 (0.6%)	0 (-)
Splintered piece	9 (3.0%)	1 (0.4%)	0 (-)	0 (-)	5 (8.6%)
Truncation	7 (2.3%)	2 (0.8%)	0 (-)	1 (0.6%)	2 (3.4%)
Undet. retouched tool	0 (-)	2 (0.8%)	0 (-)	0 (-)	0 (-)
Total	305	264	120	156	58

Undet. stands for Undetermined

Table 7 Presence (Yes) and absence (No) of cortical remains in both blanks and tools across the studied assemblages

Blanks	A2int	A2ext	A1ext	A1east	D3b alpha
No	2894 (81.4%)	1591 (83.3%)	509 (85.0%)	588 (80.0%)	245 (78.3%)
Yes	663 (18.6%)	320 (16.7%)	90 (15.0%)	147 (20.0%)	68 (21.7%)
Tools					
No	253 (83.5%)	248 (94.3%)	111 (93.3%)	147 (95.5%)	45 (83.3%)
Yes	50 (16.5%)	15 (5.7%)	8 (6.7%)	7 (4.5%)	9 (16.7%)

Percentages are provided in brackets

Table 8 Technological classification of core types identified across the studied assemblages

Classification	A2int	A2ext	A1ext	A1east	D3b alpha
Initial	8 (32.0%)	1 (8.3%)	0 (-)	4 (18.2%)	2 (20.0%)
Carinated	1 (4.0%)	1 (8.3%)	0 (-)	1 (4.5%)	4 (40.0%)
Narrow-sided	4 (16.0%)	0 (-)	1 (50.0%)	2 (9.1%)	1 (10.0%)
Semicircumferential	1 (4.0%)	5 (41.7%)	1 (50.0%)	4 (18.2%)	1 (10.0%)
Wide-faced	1 (4.0%)	1 (8.3%)	0 (-)	1 (4.5%)	0 (-)
Multi-platform	3 (12.0%)	1 (8.3%)	0 (-)	4 (18.2%)	1 (10.0%)
Flake core	2 (8.0%)	0 (-)	0 (-)	4 (18.2%)	1 (10.0%)
Tested raw material	0 (-)	0 (-)	0 (-)	1 (4.5%)	0 (-)
Shatter	5 (20.0%)	3 (25.0%)	0 (-)	1 (4.5%)	0 (-)
Total	25	12	2	22	10

The classification of laminar cores is based on Falcucci and Peresani (2018), who consider the location and orientation of the flaking surface in relation to the striking platform/s. The table also includes flake cores, tested raw materials, and core shatters. Percentages are given in brackets. One initial core in A2int is an initial carinated core. One narrow-sided core in A1ext and one in A1east can be further classified as a multiple burins

Insights from the Core Assemblage

The core assemblage is classified in Table 8. The total number of cores is not particularly high, especially in A1ext,

where only two cores have been identified. Core shatters are well-represented in A2int and A2ext. Platform cores oriented along the longitudinal axis of the core blank are the most common category in A2int and A1east. In A2int,

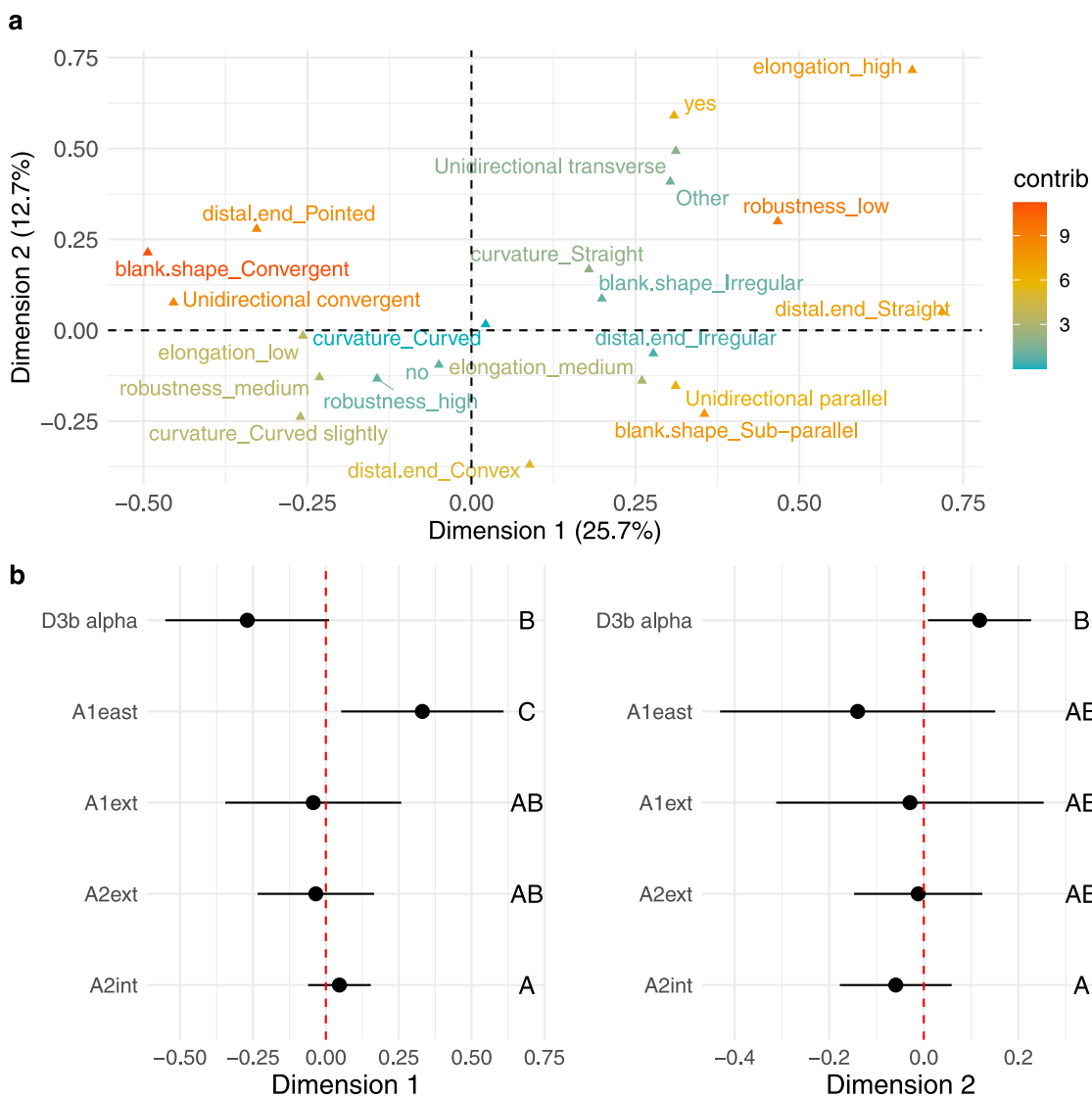


Fig. 13 Results of the Multiple Correspondence Analysis (MCA). **a** Plot of the first two dimensions of the MCA performed on complete bladelets. The color ramp indicates the contribution (as a percentage) of the variable categories to the definition of the dimensions; **b** Multi-

comparison bootstrap ANOVA on the first (left) and second (right) dimensions. Error bars represent a 95% confidence interval from the mean. Contexts sharing the same letters do not exhibit statistically significant differences (p -value < 0.05)

most of the laminar cores display the flaking surface on the narrow side of the core blank, whereas semicircumferential cores are more frequently observed in A2ext, A1ext, and A1east.

The technological characteristics of the blade and bladelet cores at Fumane have been thoroughly described by Falucci and Peresani (2018), who noted significant similarities in the reduction procedures applied across different core types. Similarly, Lombao et al. (2023) have shown that the technological and morphological classification of blade and bladelet cores is often influenced by the intensity of core reduction (see also below). Regarding blank production, most cores display bladelet negatives (Table S16), with exclusive blade

production only observed in A2int ($n = 1$) and D3b alpha ($n = 1$). Cores producing both blades and bladelets are more common in A1east, A2ext, and A2int, whereas only one core from D3b alpha shows both blade and bladelet negatives at discard.

The most significant difference in the core assemblage is the increased presence of carinated cores in D3b alpha (Fig. 14 and SM Fig. S31), a pattern linked to more independent bladelet production at other Aurignacian sites (Falucci et al., 2024). SM Figure S32 demonstrates a strong correspondence between the lengths of the flaking surfaces on carinated cores and the lengths of complete bladelets in D3b alpha, further supporting the use of carinated

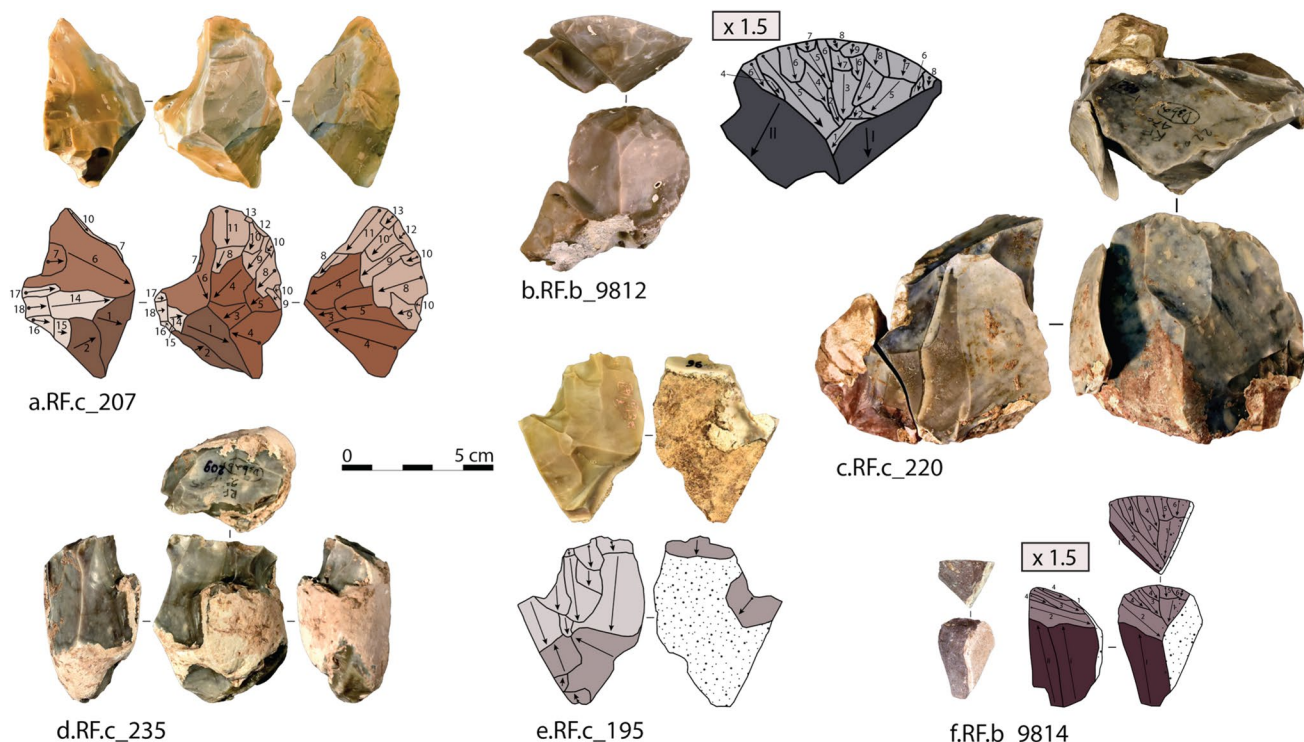


Fig. 14 Example of cores recovered from D3b alpha. Artifacts **a**, **b**, and **f** are carinated cores; **a** can be further classified as a thick-nosed endscraper, while **b** and **f** are carinated endscrapers; **c** is a semicircumferential core with a few refitted blanks; **d** is an initial core from a small nodule; **e** is a flake core with unidirectional removals. **a**, **b**, **e**, and **f** are complemented by diacritic drawings that display the reduction phases (darker colors indicate earlier phases, while lighter colors represent later phases of blank removal). The direction of removals is shown by arrows, and the presumed order of removals is indicated by numbers. The diacritic drawings of **b** and **f** are enlarged by 1.5 times to enhance readability. Each artifact is accompanied by its ID, as listed in the dataset published in this paper and the 3D dataset published by Falcucci and Peresani (2023). The other carinated endscraper from D3b alpha is presented in SM Fig. S31

represent later phases of blank removal). The direction of removals is shown by arrows, and the presumed order of removals is indicated by numbers. The diacritic drawings of **b** and **f** are enlarged by 1.5 times to enhance readability. Each artifact is accompanied by its ID, as listed in the dataset published in this paper and the 3D dataset published by Falcucci and Peresani (2023). The other carinated endscraper from D3b alpha is presented in SM Fig. S31

technology in this SU. Carinated cores from the A2 and A1 subsets sum to a total of 4 items (SM Fig. S33), of which one is classified as initial carinated core due to the few removals visible aimed at shaping the flaking surface's convexities.

Typological Variability between and within Stratigraphic Units

The most prevalent tools across the Aurignacian sequence at Fumane are retouched bladelets, with their proportions ranging from 57 to 86% (Table 6). Notably, their frequency is reduced in both A2int and D3b alpha. While the diminished number of retouched bladelets in A2int may be attributed to different spatial usage during the formation of A2 (see the “On the Variability of the Selected Subsets and Future Research Directions” section), the decrease in D3b alpha aligns with findings from Falcucci et al. (2020). That study also observed an increase in the number of endscrapers towards the top of the Aurignacian sequence. In D3b alpha, carinated cores (see

Fig. 14 and SM Fig. S31) can be further categorized into carinated endscrapers ($n=3$) and thick-nosed endscrapers ($n=1$). Other diagnostic tools of the Aurignacian, such as Aurignacian blades, are nearly absent, with just one example found in A1east. Burins, on the other hand, are present across all studied assemblages, especially in A2int and A2ext.

Regarding retouched bladelets, the size variations between the A2–A1 subsets and D3b alpha are consistent with the blank analysis, showing that bladelets from D3b alpha are smaller in all linear dimensions. Conversely, retouched bladelets from A1east do not differ significantly from those in A2int, A2ext, and A1ext (SM Figs. S34–S35). Most bladelets were modified using marginal retouching, with variability in the application of alternate, direct, and inverse retouching techniques. While inverse retouching remains relatively consistent, the ratio between alternate and direct retouching varies considerably (SM Fig. S36). Notably, direct retouching is more common in D3b alpha, where it accounts for 50% of all retouched bladelets.

Further Insights from the Raw Material Variability and Reduction Intensity Proxies

Several factors may explain the observed techno-typological variability across the studied assemblages. While chrono-cultural shifts are a crucial aspect to consider (see the “The Development of the Aurignacian in Northeastern Italy and its Wider Implications” section), other factors are likely contributing to the identified differences. In some cases, the variation is more pronounced when considering spatial components rather than stratigraphic patterns. To further explore the potential roles of the use of space and mobility strategies, we analyzed raw material variability and applied two methods to quantify the reduction intensity of the analyzed subsets.

All assemblages are characterized by the use of high-quality cherts from the Maiolica, Scaglia Rossa, and Scaglia Variegata formations, which were available within a 5 km radius of Fumane (Bertola, 2001; Delpiano et al., 2018). Maiolica is the most frequently used raw material type across blanks, tools, and cores (SM Tables S17–S20). In terms of blanks, Maiolica accounts for 90% in D3b alpha, while in other assemblages, it ranges between 67% (A2ext) and 77% (A1ext). This proportion slightly decreases among the tools. When comparing retouched bladelets to other tools (e.g., endscrapers, burins, retouched flakes, and retouched blades), Maiolica is less common in retouched bladelets in A2ext, A1ext, A1east, and especially in D3b alpha. However, in A2int, retouched bladelets are predominantly made from Maiolica (see SM Table S18).

The SDI performed on laminar cores suggests that cores in D3b alpha are less reduced compared to other SUs. This trend is partially observed in A2int, although a more balanced distribution pattern is evident (SM Fig. S37). For carinated cores, defining reduction intensity is more complex due to their lower numbers in A2int–A1east. However, in D3b alpha, carinated cores seem to be more reduced compared to other platform cores within the same SU (SM Fig. S38). When combining SDI results with the ratios between the Minimum Number of Flaked Products (MNFPs) and the total number of cores, D3b alpha shows the lowest

Table 9 Minimum Number of Flaked Products (MNFPs) to cores ratios across the studied assemblages

Assemblage	MNFPs	Cores	MNFP-to-Core-Ratio
D3b alpha	202	10	20.2
A1east	450	22	20.45
A1ext	337	2	168.5
A2ext	1006	12	83.83
A2int	1832	25	73.28

The MNFP includes both blanks and tools

value, closely followed by A1east (Table 9). Additionally, the blanks-to-tools ratio based on MNFPs (Table 10) suggests more intense tool manufacturing activity and/or discard in the external area of the cave, with particularly low ratios when bladelets are separated from other tool blanks.

Osseous Tools and Personal Ornaments

In addition to lithics, the studied samples contain a varying number of osseous tools and personal ornaments. Osseous tools are generally scarce and completely absent in A1ext (Table 11). Awls and pointed tools made from bone were recovered in A2int and A2ext, while antler tools were found in A2int, A1east, and D3b alpha. In A2int, these antler tools can be broadly classified as points, although they lack diagnostic features to be further categorized as either split-based or massive-based points (Doyon, 2020). An antler point found in A1east exhibits a fracture at its base, though it remains undetermined if this was intentional. D3b alpha contains a complete split-based point, discovered in square 66, near a similar point found in D3b (Broglio & Dalmeri, 2005). The D3b split-based point was located in square 65, adjacent to the first square meters where D3b alpha was identified. Owing to the strong similarity between the two points (Broglio & Dalmeri, 2005), this might indicate that D3b alpha extended, at least partially, towards the eastern

Table 10 Ratios of blanks to tools, based on the Minimum Number of Flaked Products (MNFPs) only, across the studied assemblages

Assemblage	Blanks	Tools	Blank-to-Tool-Ratio
D3b alpha	172	30	5.73
A1east	392	58	6.76
A1ext	294	43	6.68
A2ext	896	110	8.14
A2int	1702	130	13.1

Table 11 Bone and antler tools recovered across the investigated areas and stratigraphic units

	A2int	A2ext	A1ext	A1east	D3b alpha
Bone	1	3	-	-	-
Awl		2			
Pointed tool	1	1			
Antler	2	-	-	1	1
Point	1			1	
Point, probable	1				
Split-based point					1
Total	3	3	-	1	1

The artifact classified as *Point, probable* is a mesial fragment

side of the cave, though further spatial analyses and technological refits are needed to confirm this.

Regarding ornamental objects, Fumane is renowned for its abundance of marine and freshwater shells (Peresani et al., 2019a). The frequency of these shells is very low in all external SUs, never exceeding four artifacts (Table 12). In contrast, A2int contains a large sample of shells, representing various taxa. The most common are *Homalopoma sanguineum*, followed by *Nassarius* sp., *Cyclope* sp., and *Clanculus* sp. Finally, the only grooved deer incisor recovered in the studied subsamples belongs to A1east.

Discussion: Part Two

On the Variability of the Selected Subsets and Future Research Directions

The renewed technological study of selected subsets from different excavation areas at Fumane offers a compelling illustration of the complexity of Pleistocene cave sites. The A2 and A1 subsets show overall consistency in the organization of the lithic technology but reveal notable variability in the frequency of specific blank classes and tools, especially those crucial for understanding core reduction procedures and curation strategies. Our results show that all sampled excavation areas provide valuable insights into the spatial organization of the site during the formation of the Aurignacian palimpsest.

The lithic analysis largely confirms the prior technological definition of the Protoaurignacian at Fumane (Falcucci, 2018), offering new quantitative data to support findings

Table 12 Symbolic artifacts recovered across the investigated areas and stratigraphic units

	A2int	A2ext	A1ext	A1east	D3b alpha
Shells	98	3	4	3	1
<i>Bittium</i>	5				
<i>Clanculus</i>	13				
<i>Cyclope</i>	16		1	3	
<i>Glycymeris</i>	2				
<i>Homalopoma</i>	35	1	1		1
<i>Nassarius</i>	17	2			
<i>Ocinebrina</i>	2				
<i>Phorcus</i>	2				
Other	6		2		
Misc. artifacts	-	-	-	1	-
Deer incisor				1	
Total	98	3	4	4	1

Shells are sorted according to genus. The *Other* group include genera that are found only once (i.e., *Cerithium*, *Euspira*, *Papillocardium*, *Rissoa*, *Trivia*, *Clanculus*, *Jujubinus*, and a Gastropod). *Misc.* stands for Miscellaneous

on lithic technology and human behavior during the early Upper Paleolithic south of the Alps. Previous studies on the chrono-cultural development of the Aurignacian at Fumane tended to exclude the cave interior due to the increased post-depositional processes observed in that area (Falcucci et al., 2020). However, our results indicate that this area is crucial for understanding site occupation patterns, particularly evident in the square meters identified through our spatial analysis. Although inter-SU connections were recorded in this area, the technological study suggests that the observed variability is not attributable to post-depositional processes involving significant artifact migration from underlying and overlying SUs.

This hypothesis is supported by the absence of lithics linked to the underlying Uluzzian and Mousterian SUs. For instance, the bipolar technique, commonly associated with the Uluzzian from SU A3 (Peresani et al., 2016), and flakes and cores linked to Mousterian Levallois technology (Peresani, 2012), were not identified in our study. As an example, many of the flakes in A2int are associated with the initialization and maintenance of blade-bladelet cores. Similarly, the similarity in the morphometric and technological features of the bladelets from A2int and A2ext does not suggest significant downward material movement from the D sedimentary body. It is worth noting that the D3b alpha lithic technology is oriented towards carinated technology, which is rarely used in A2int.

We hypothesize that the variability between the internal and external areas of the cave may result from some degree of organization of the living space, which persisted throughout the deposition of the Protoaurignacian palimpsest. Considering all available data, it is conceivable that while core reduction may have occurred in both the internal and external areas of the cave, the variability in the frequency of blanks, tools, and cores, as well as reduction intensity patterns, suggests that Protoaurignacian foragers organized space according to different activities. This is particularly evident when considering the high prevalence of retouched bladelets in A2ext, indicating that tool retouching and the refurbishing of multi-component tools were more commonly conducted in the external area of the cave, as noted by Broglio et al. (2005). Conversely, the higher number of flakes and endscrapers in the cave interior might indicate space used for activities such as hide working, as supported by the functional analyses by Aleo et al. (2021).

Our results highlight the importance of basing interpretations of site use strategies on the largest attainable excavation surface to minimize information loss. At Fumane this is possible thanks to the extensive archaeological excavations that have covered a significant portion of the space likely occupied by foraging groups during the accumulation of the Protoaurignacian. We found no strong evidence supporting the hypothesis of recurrent disposal of knapping by-products

in the cave's northeastern side. For instance, if this were the case, we would expect to find a higher proportion of blanks belonging to the initialization and maintenance phases in these areas compared to the cave exterior. Instead, blanks with cortical remains are evenly distributed between A2int and A2ext, and cores show similar reduction intensity distributions. Some displacement of lithics due to syn-depositional processes, such as trampling, remains a more plausible explanation (Broglio & Dalmeri, 2005), as suggested by the identified break connections.

The re-analysis of A1 is also significant. The lithic technology of both A1ext and A1east is distinctly Protoaurignacian, with the differences from the A2 subsamples not indicative of a cultural shift, consistent with the previous techno-typological study (Falcucci et al., 2020). The only notable difference—namely, the production of longer bladelets in A1east—may reflect a remarkable example of inter-knapper variability or spatially localized activities with minimal diachronic significance. These findings support the spatial analysis of the break connections and strongly suggest that A2 and A1 should be considered part of the same Protoaurignacian palimpsest.

This preliminary discussion presents intriguing avenues for future research at the site. While the break connection study has helped assess the sequence's integrity in selected excavation areas, future investigations could benefit from implementing technological refitting. This would enable further exploration of space organization during the A2–A1 palimpsest's formation and assess the degree of contemporaneity between artifact accumulations in different cave areas (Romagnoli et al., 2018; Vaquero et al., 2019). Additionally, zooarchaeological investigations should consider this spatial variation to provide further evidence complementing lithic analysis results. Refitting broken bones could determine if lithic and bone connections exhibit different spatial distributions, contributing to a more comprehensive understanding of formation processes in relation to human, animal, and natural activities at the site (Vaquero et al., 2017). Furthermore, future radiocarbon assessments should test intra-site variability by sampling areas identified through the spatial analysis of break connections.

Overall, our study confirms that A2–A1 represents a palimpsest of recurrent and intense site occupation, unlikely to be subdivided further due to the lack of consistent spatial data across the excavation area. On the other hand, evidence of a short-term occupation can be identified in the thin SU D3b alpha. The low density of finds, coupled with the almost exclusive use of locally available raw materials, which were less reduced compared to the A2–A1 Protoaurignacian, suggests a shift in mobility strategies during D3b alpha's formation.

It is intriguing that D3b alpha dates to the Heinrich Event 4, detected at Fumane based on a shift to colder conditions

and reduced vegetation cover (López-García et al., 2015), as well as by the dating of this SU itself. The zooarchaeological assessment by Marín-Arroyo et al. (2023) suggests that the foragers responsible for D3b alpha's archaeological material accumulation focused more on hunting montane-adapted animals, with a decrease in red deer presence. Combining the available data, it is plausible that D3b alpha records a reorganization of foraging mobility in the region, with increased residential mobility. This hypothesis aligns with Moreau et al. (2015), who proposed similar changes in mobility strategies for sub-contemporary Aurignacian sites in northeastern Mediterranean Europe.

The Development of the Aurignacian in Northeastern Italy and its Wider Implications

The intra-SU and spatial variability observed at Fumane opens new research avenues to better understand the site's use during the formation of the A2–A1 palimpsest. The diachronic analysis, instead, allows us to reject the hypothesis that the Protoaurignacian continued into the Early Aurignacian time-frame in northeastern Italy (see Falcucci et al., 2020). While all studied subsets from SUs A2 and A1 are characterized by the production of slender and straight blanks often modified into Dufour sub-type Dufour bladelets (Demars & Laurent, 1992), the differences identified in D3b alpha reflect a shift to the Early Aurignacian technological system.

This interpretation is consistent with technological and chronological data from other European sites (Barshay-Szmidt et al., 2018; Talamo et al., 2012; Wood et al., 2014). Technologically, the Early Aurignacian is primarily associated with the production of short, non-twisted bladelets detached from wide-front carinated cores, a reduced emphasis on modifying bladelets through marginal retouching, and the independent production of robust blades (Dinnis et al., 2019; Teyssandier & Zilhão, 2018). These features, while not exclusive to the Early Aurignacian, represent behavioral tendencies within the broader and relatively homogeneous techno-typological system that defines the Aurignacian technocomplex as a whole (Bataille et al., 2018; Falcucci et al., 2017).

A notable feature of the shift from the Protoaurignacian to the Early Aurignacian is the increased use of carinated technology, leading to a marked dissociation in the production of blades and bladelets. This technological shift is evident across Europe at stratified sites such as Le Piage (Bordes, 2006), Isturitz (Normand, 2006), Labeko Koba (Arrizabalaga & Altuna, 2000), La Viña (Santamaría, 2012), and Les Cottés (Roussel et al., 2016), among others. At Fumane, the lithic evidence is further supported by the discovery of a split-based antler point in D3b alpha, a tool considered diagnostic of the Early Aurignacian (Doyon, 2020; Tejero & Grimaldi, 2015; Teyssandier & Zilhão, 2018). In this regard, Banks et al. (2013a) suggest that osseous tools are more

effective for identifying chrono-cultural changes because, unlike lithics, they are less influenced by variations in site use and function.

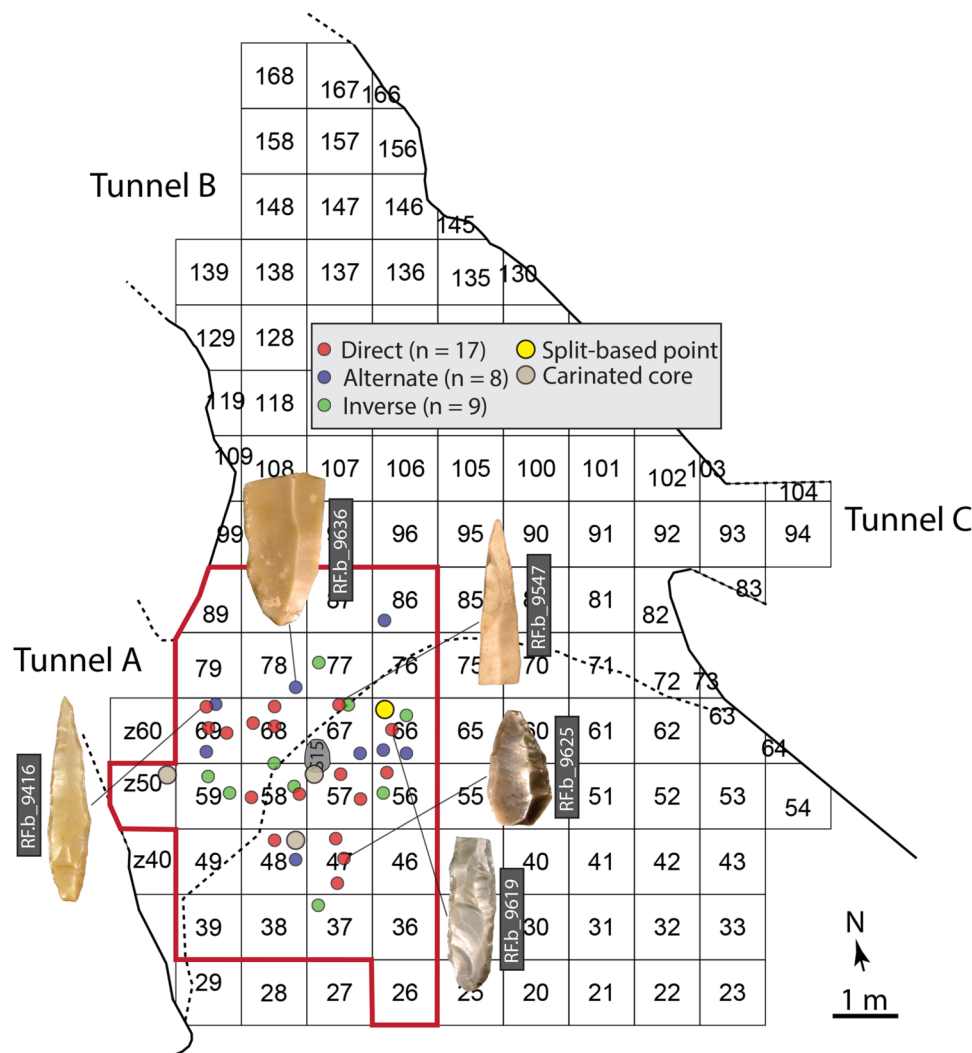
The Early Aurignacian of D3b alpha also exhibits specific features that differ from other Early Aurignacian assemblages described in the Aquitaine region (Bordes, 2006) and the Swabian Jura (Conard & Bolus, 2006). In terms of lithic technology, we did not identify the production of robust blades or the transport of blades modified by Aurignacian retouch, such as the so-called strangulated blades. However, this may be linked to the marked reliance on locally available high-quality raw materials at Fumane and different mobility strategies in the region.

The bladelets in D3b alpha frequently exhibit marginal retouching, which is uncommon for bladelets from other Early Aurignacian sites north of the Alps. When comparing the size and retouch positions of the D3b alpha bladelets with those from the underlying A2–A1 (see the “Typological Variability between and within Stratigraphic Units” section),

it seems unlikely that the presence of retouched bladelets in D3b alpha can be attributed solely to stratigraphic mixing or excavation errors. Our analyses indicate that the retouched bladelets in D3b alpha are notably smaller and are more frequently modified by direct retouching. To further investigate this, we plotted all retouched bladelets from D3b alpha, categorizing them by retouch position. As shown in Fig. 15, there is no clear spatial clustering of retouched bladelets within this SU, nor is there a separation between bladelets with alternate or inverse retouch and those with direct retouch. Notably, retouched bladelets from D3b alpha were recovered from 14 different square meters, with many located near feature S15, as well as in proximity to the split-based antler point and the carinated cores.

Despite this, we cannot entirely rule out the possibility that some retouched bladelets infiltrated into D3b alpha from the underlying Protoaurignacian SUs, particularly given the few conjoins identified between A2 and D3b alpha. However, it is noteworthy that several retouched bladelets

Fig. 15 Spatial distribution of retouched bladelets in D3b alpha, categorized by retouch position. The figure also shows the locations of the split-based point, carinated cores, and feature S15. As discussed in the “Materials and Methods” section, we randomized the XY coordinates of the retouched bladelets within the sub-square meter grid. One carinated core is not plotted due to the absence of precise square meter data in the dataset, although it is known to originate from the area near S15. The red outline indicates the portion of D3b alpha sampled in our technological study (see also SM Fig. S15b). Representative photographs of the retouched bladelets are included, with tool IDs corresponding to those listed in the associated dataset



were found below the drip line, where post-depositional processes had less impact compared to the cave interior. Furthermore, areas identified as susceptible to significant post-depositional disturbance, according to the SFR (see Fig. 10), do not contain more retouched bladelets than other square meters. For instance, square 77 contains only a single retouched bladelet. These lines of evidence suggest that post-depositional processes and excavation errors may not fully account for the presence of retouched bladelets in D3b alpha. This supports our hypothesis that the lateral modification of bladelets, particularly through direct retouch, was part of the technological behavior of the foraging groups responsible for the formation of the D3b alpha assemblage, although it was less commonly used compared to the preceding Protoaurignacian.

The modification of bladelets by marginal retouching might be a defining characteristic of the first Early Aurignacian in Italy. For example, at Castelcivita in southern Italy, Falcucci et al. (2024) identified a rapid shift from the Protoaurignacian to the Early Aurignacian just before the Campanian Ignimbrite super-eruption. This shift is marked by the use of carinated technology, which is associated with the frequent modification of miniaturized bladelets through direct bilateral retouching, a pattern also observed at Fumane. It is however worth noting that later Early Aurignacian sites in Italy, such as Riparo Mochi (Laplace, 1977) and Grotta della Cala (Benini et al., 1997), are characterized by a significant decrease in the proportion of retouched bladelets, possibly indicating internal chronological variation within the Early Aurignacian that merits further investigation.

The differences observed between the Italian Early Aurignacian and sites north of the Alps cannot be attributed to the cultural isolation of foraging groups in Italy. This is evidenced by data on the circulation of raw materials, which were collected in central Italy and southeastern France and transported over several hundred kilometers along the Tyrrhenian coastline (Grimaldi et al., 2014; Riel-Salvatore & Negrino, 2018b). Additionally, evidence of contact throughout the Aurignacian period between regions northeast and south of the Alps is supported by finds such as Mediterranean shells recovered in Lower Austria (Strobl & Obermaier, 1909). Interestingly, the existence of regional social networks among European foraging groups has been identified through the use of personal ornaments made from various raw materials (Vanhaeren & d'Errico, 2006). This aspect warrants further investigation using isolation-by-distance models, as recently applied to the Gravettian (Baker et al., 2024).

The hypothesis of a marked continuity of the Protoaurignacian technological system in northern Italy now primarily rests on evidence from the site of Riparo Bombrini. According to Riel-Salvatore and Negrino (2018a), the Protoaurignacian at Bombrini spans from approximately 41 to 36 ka cal

BP. However, the available radiocarbon dates (Benazzi et al., 2015) have recently been scrutinized by Frouin et al. (2022), who noted that the two dated bone samples from the Protoaurignacian SUs A2 and A1 had low collagen content and might be contaminated, as indicated by high C:N ratios (see also Zilhão et al., 2024). The data from Bombrini also contrast with the nearby site of Mochi, where the Protoaurignacian is significantly older and is followed by an Early Aurignacian component (Tejero & Grimaldi, 2015). However, Mochi cannot currently be considered a key site for understanding the development of the Aurignacian in northwestern Italy. This is because the thick Aurignacian deposit, which spans approximately 1.5 m, has yet to be analyzed through a technological lens, particularly the thick SU F (Laplace, 1977). Moreover, Bayesian models by Douka et al. (2012) and Frouin et al. (2022) suggest that there may be some chronological subdivision within SUs G and F (e.g., G51) that have yet to be fully understood.

Conclusions

In this study, our primary focus was to evaluate the integrity of the Aurignacian assemblages at Fumane Cave in northeastern Italy. Our aim was to establish a robust framework for conducting new high-resolution studies of chrono-cultural variability at both the site and regional levels, while also identifying areas for future examination to better understand intra-site variability in the use of space by early *Homo sapiens* foraging groups in northeastern Italy. Central to our methodology was the implementation of a meticulous experimental protocol aimed at identifying break connections between blade fragments. This protocol, which has proven reliable and highly effective in our case study, offers promising applications for other key sites. By employing this systematic approach, researchers can identify excavation areas prone to integrity issues which might bias chrono-cultural studies, especially in the complex formation processes of karstic cave sites.

At Fumane, we demonstrated the overall integrity of the Protoaurignacian stratigraphic units A2 and A1, which have been instrumental in shaping our understanding of the European Protoaurignacian over the years. Likewise, post-depositional processes appear to have minimally impacted the displacement of lithic artifacts across the stratigraphic sequence, with vertical displacement being negligible in most cases. However, our analysis revealed a clear interrelation between A2 and A1, as for example illustrated by the high number of short and medium conjoining links connecting the two stratigraphic units. Based on these observations and the results of the technological study, we argue that A2 and A1 should be considered a single analytical unit when investigating the Protoaurignacian at the site, as previously proposed by Falcucci et al.

(2017). The Protoaurignacian palimpsest does likely include A2R, excavated in the innermost area of the cave, which was frequently intertwined with A2 as per the field observations. However, we excluded A2R from our technological analysis because it did not meet our criteria for integrity.

Furthermore, the technological study of the subsets from A2 and A1 revealed that the variability observed between different areas of A2, as well as in the eastern portion of A1, likely reflects the spatial organization of activities as well as knapper-related variability during the formation of the Protoaurignacian sedimentary body. This suggests that (1) restricting analysis solely to the cave exterior may not capture the full extent of human activities at the site, and (2) the confounding effects of spatial organization and individual knapping variability should be considered when discussing cultural variability at Fumane and other Paleolithic sites.

Regarding the upper part of the Aurignacian sequence, our break connection search and subsequent spatial analysis did not definitively demonstrate the integrity of the lithic assemblages, as many SUs described during excavation contain a high frequency of inter-stratigraphic connections. Only the thin stratigraphic unit D3b alpha, dated to the timeframe of Heinrich Event 4, could be reliably used to detect chrono-cultural changes in the Aurignacian sequence of Fumane. Our examination of D3b alpha led us to reject the hypothesis of chrono-cultural continuity of the Protoaurignacian at the site, reassigning it to the Early Aurignacian, while dismissing a previous correlation with D3d. However, it should be noted that the occupation intensity at the site was low during the formation of the D3 complex, and numerical differences between the compared assemblages warrant caution.

The new techno-typological study of the Early Aurignacian from D3b alpha aligns the sequence of Fumane with the broader pan-European understanding of the early development of the Upper Paleolithic, while highlighting certain variability that suggests regional differences across the wide geographical range of the Aurignacian. The most notable difference is the use of marginal retouching to modify the morphology of bladelets, which however appears less common than in the underlying Protoaurignacian from A2–A1. While we cannot rule out the possibility that some bladelets result from minor mixing between D3b alpha and the Protoaurignacian sedimentary body below, several technological and typological features of these bladelets support the use of marginal retouching to modify bladelets in the Early Aurignacian at Fumane.

Overall, this study highlights the challenges of using the layers defined during archaeological fieldwork as analytical units for identifying cultural changes and modeling chronological boundaries at multi-stratified sites. We have demonstrated that some of these units lack clear stratigraphic value. Future studies at the site should approach A2 and A1 not as chronologically distinct stratigraphic units but as

components of a palimpsest formed by multiple occupations and activities that are complex to disentangle. Similarly, the numerous inter-stratigraphic connections between A2–A1 and the overlying SUs from the D-complex underscore the expected stratigraphic fuzziness of cave sites. This fuzziness results from syn- and post-depositional disturbances and localized excavation errors, especially in the absence of sterile layers between successive human occupations. This issue is not unique to Fumane but is common across many cave sites. Thus, this study serves as a critical reference for prompting renewed chronological and techno-typological reassessments at numerous Pleistocene stratified sites.

Supplementary Information The online version contains supplementary material available at <https://doi.org/10.1007/s41982-024-00203-0>.

Acknowledgements We want to acknowledge all the researchers and students involved in the recovery, preparation, and study of the archaeological record from Fumane Cave. We also wish to thank Arianna Cocirova and Davide Delpiano for participating in some break connection sessions. We are grateful to João Zilhão and two other anonymous reviewers for their thoughtful comments. However, any shortcomings remain our own.

Author Contribution AF, DG, and MP conceptualized the study. AF designed the break connection program. AF, FZ, and MDL organized the lithic assemblages and conducted the break connection trials. AF and LC recorded thermal alterations. AF and MP reviewed the excavation documentation. DG designed and conducted the spatial analyses. AF designed and conducted the technological analyses of the lithic assemblages. AF, DG, and MP interpreted and commented on the results of the analyses. AF and DG wrote the manuscript with contributions from MP. AF revised the manuscript. AF and MP collected the funding.

Funding Open Access funding enabled and organized by Projekt DEAL. Open Access funding was supported by the DEAL agreement between Springer and the University of Tübingen. Research and fieldwork at Fumane Cave is coordinated by the University of Ferrara (M. Peresani) in the framework of a project supported by the Ministry of Culture – SAPAB Archaeological Superintendence, public institutions (Lessinia Mountain Community—Regional Natural Park, B.I.M. Adige, Fumane Municipality), private associations and companies, and in collaboration with Italian and European research centers. Research reported in this publication was supported by the Deutsche Forschungsgemeinschaft (DFG) under grant agreement no. 431809858 (project title: Investigating Early Upper Paleolithic Technological Variability and Cultural Dynamics South of the Alps; recipient: A. Falucci).

Data Availability The datasets generated and analyzed in the current study are available in the associated research compendium available on Zenodo: <https://doi.org/10.5281/zenodo.10965413>. Furthermore, the 3D models of cores used to compute the SDI are also published in Zenodo: <https://doi.org/10.5281/zenodo.6362149>. The raw data collected for this study, necessary to reproduce the reported results, is licensed, except where otherwise specified, under the CC-BY-NC-ND-4.0. All analyses were conducted in the R programming environment (Posit team, 2023; R Core team, 2022), utilizing various packages for data manipulation, visualization, and statistical analyses (Kassambara & Mundt, 2017; Kassambara, 2021; Lê et al., 2008; Oksanen et al., 2022; Wickham et al., 2019). The Aurignacian lithic assemblages from Fumane Cave are permanently stored at the University of Ferrara, Dipartimento di Studi Umanistici, Sezione di

Scienze Preistoriche e Antropologiche, Corso Ercole I d'Este, 32, I-44100 Ferrara, Italy.

Declarations

Competing Interests The authors declare no competing interests.

Open Access This article is licensed under a Creative Commons Attribution 4.0 International License, which permits use, sharing, adaptation, distribution and reproduction in any medium or format, as long as you give appropriate credit to the original author(s) and the source, provide a link to the Creative Commons licence, and indicate if changes were made. The images or other third party material in this article are included in the article's Creative Commons licence, unless indicated otherwise in a credit line to the material. If material is not included in the article's Creative Commons licence and your intended use is not permitted by statutory regulation or exceeds the permitted use, you will need to obtain permission directly from the copyright holder. To view a copy of this licence, visit <http://creativecommons.org/licenses/by/4.0/>.

References

- Aleo, A., Duches, R., Falcucci, A., Rots, V., & Peresani, M. (2021). Scraping hide in the early Upper Paleolithic: Insights into the life and function of the Protoaurignacian endscrapers at Fumane Cave. *Archaeological and Anthropological Sciences*, 13, 137. <https://doi.org/10.1007/s12520-021-01367-4>
- Anderson, L., Bon, F., Bordes, J.-G., Pasquini, A., Slimak, L., & Teyssandier, N. (2015). Relier des espaces, construire de nouveaux réseaux : aux origines du Protoaurignacien et des débuts du Paléolithique supérieur en Europe occidentale. In Naudinot, N., Meignen, L., Binder, G. et al. (eds.): Les systèmes de mobilité de la Préhistoire au Moyen Âge XXXVe rencontres internationales d'archéologie et d'histoire d'Antibes, pp. 57–73. Éditions APDCA, Antibes.
- Anderson, L., Lejay, M., Brugal, J.-P., Costamagno, S., Heckel, C., de Araujo Igreja, M., Pradeau, J.-V., Salomon, H., Sellami, F., Théry-Parisot, I., Barshay-Szmidt, C., Mensan, R., & Bon, F. (2018). Insights into Aurignacian daily life and camp organization: The open-air site of Régismont-le-Haut. *Quaternary International*, 498, 69–98. <https://doi.org/10.1016/j.quaint.2018.04.034>
- Andrefsky, W. (1998). *Lithics: Macroscopic approaches to analysis*. Cambridge University.
- Arrizabalaga, A. & Altuna, J. (2000). Labeko Koba (País Vasco). Hienas y humanos en los albores del Paleolítico superior. *Munibe*, 52, 935.
- Bachellerie F. (2011). Quelle unité pour le Châtelperronien ? Apport de l'analyse taphonomique et techno-économique des industries lithiques de trois gisements aquitains de plein air : le Basté, Bidart (Pyrénées-Atlantiques) et Canaule II (Dordogne) Ph.D. Dissertation, Université Bordeaux I.
- Bailey, G. (2007). Time perspectives, palimpsests and the archaeology of time. *Journal of Anthropological Archaeology*, 26, 198–223. <https://doi.org/10.1016/j.jaa.2006.08.002>
- Baker, J., Rigaud, S., Pereira, D., Courtenay, L. A., & d'Errico, F. (2024). Evidence from personal ornaments suggest nine distinct cultural groups between 34,000 and 24,000 years ago in Europe. *Nature Human Behaviour*. <https://doi.org/10.1038/s41562-023-01803-6>
- Banks, W. E., d'Errico, F., & Zilhão, J. (2013a). Human-climate interaction during the Early Upper Palaeolithic: Testing the hypothesis of an adaptive shift between the Proto-Aurignacian and the Early Aurignacian. *Journal of Human Evolution*, 64, 232–232. <https://doi.org/10.1016/j.jhevol.2013.01.001>
- Banks, W. E., d'Errico, F., & Zilhão, J. (2013). Revisiting the chronology of the Proto-Aurignacian and the Early Aurignacian in Europe: A reply to Higham et al.'s comments on Banks et al. (2013). *Journal Of Human Evolution*, 65, 810–817. <https://doi.org/10.1016/j.jhevol.2013.08.004>
- Barshay-Szmidt, C., Normand, C., Flas, D., & Soulier, M.-C. (2018). Radiocarbon dating the Aurignacian sequence at Isturitz (France): Implications for the timing and development of the Protoaurignacian and Early Aurignacian in western Europe. *Journal of Archaeological Science : Reports*, 17, 809–838. <https://doi.org/10.1016/j.jasrep.2017.09.003>
- Barton, C. M., & Clark, G. A. (1993). Cultural and natural formation processes in late Quaternary cave and rockshelter sites of western Europe and the Near East. In P. Goldberg, D. T. Nash, & M. Petraglia (Eds.), *Formation processes in archaeological context* (Vol. 17, pp. 33–60). Madison: Prehistory Press.
- Bataille, G., Tafelmaier, Y., & Weniger, G.-C. (2018). Living on the edge – A comparative approach for studying the beginning of the Aurignacian. *Quaternary International*, 474, 3–29. <https://doi.org/10.1016/j.quaint.2018.03.024>
- Bel, M. Á. (2022). Lithic taphonomy and the use of the spatial information: Assessing Palaeolithic sequence of Cova de les Cendres (Teulada-Moraira, Spain). *Archaeological and Anthropological Sciences*, 14, 173. <https://doi.org/10.1007/s12520-022-01642-y>
- Bel, M. Á., Martínez-Alfaro, Á., & Villaverde, V. (2020). Refitting lithic laminar fragments to assess Palaeolithic sequences: The case of Cova de les Cendres (Teulada-Moraira, Alicante, Spain). *Quaternary International*, 566–567, 152–162. <https://doi.org/10.1016/j.quaint.2020.04.023>
- Benazzi, S., Slon, V., Talamo, S., Negrino, F., Peresani, M., Bailey, S. E., Sawyer, S., Panetta, D., Vicino, G., Starnini, E., Mannino, M. A., Salvadori, P. A., Meyer, M., Paabo, S., & Hublin, J. J. (2015). The makers of the Protoaurignacian and implications for Neandertal extinction. *Science*, 348, 793–796. <https://doi.org/10.1126/science.aaa2773>
- Benini, A., Boscato, P., & Gambassini, P. (1997). Grotta della Cala (Salerno): Industrie litiche e faune uluzziane ed aurignaziane. *Rivista di Scienze Preistoriche*, 48, 37–95.
- Benito-Calvo, A., Martínez-Moreno, J., Mora, R., Roy, M., & Roda, X. (2011). Trampling experiments at Cova Gran de Santa Linya, Pre-Pyrenees, Spain: Their relevance for archaeological fabrics of the Upper-Middle Paleolithic assemblages. *Journal of Archaeological Science*, 38, 3652–3661. <https://doi.org/10.1016/j.jas.2011.08.036>
- Benn, D. (1994). Fabric shape and the interpretation of sedimentary fabric data. *Journal of Sedimentary Research*, 64, 910–915. <https://doi.org/10.1306/d4267f05-2b26-11d7-8648000102c1865d>
- Bertola, S. (2001). Contributo allo studio del comportamento dei primi gruppi di Homo sapiens diffusi in Europa. Sfruttamento della selce, produzione dei supporti lamellari, confezione delle armature litiche nel sito aurignaziano della Grotta di Fumane nei Monti Lessini (Verona). Ph.D. Dissertation, University of Bologna.
- Bertola, S., Broglio, A., Cristiani, E., De Stefani, M., Gurioli, F., Negrino, F., Romandini, M., & Vanhaeren, M. (2013). La diffusione del primo Aurignaziano a sud dell'arco alpino. *Preistoria Alpina*, 47, 17–30.
- Bivand, R. S., Pebesma, E., & Gómez-Rubio, V. (2013). Applied spatial data analysis with R. UseR!, 2nd edn. Springer. <https://doi.org/10.1007/978-1-4614-7618-4>
- Bocek, B. (1986). Rodent ecology and burrowing behavior: Predicted effects on archaeological site formation. *American Antiquity*, 51, 589–603. <https://doi.org/10.2307/281754>

- Bocek, B. (1992). The Jasper Ridge reexcavation experiment: Rates of artifact mixing by rodents. *American Antiquity*, 57, 261–269. <https://doi.org/10.2307/280731>
- Bordes, J. G. (2000). La séquence aurignacienne de Caminade révisée : l'apport des raccords d'intérêt stratigraphique. *PALEO*, 12, 387–407.
- Bordes, J.-G. (2002). Les interstratifications Châtelperronien/Aurignacien du Roc-de-Combe et du Piage (Lot, France): analyse taphonomique des industries lithiques, implications archéologiques. Ph.D. Dissertation, University of Bordeaux I.
- Bordes, J.-G. (2006). News from the West: A revaluation of the classical Aurignacian sequence of the Périgord. In O. Bar-Yosef & J. Zilhão (eds.): Towards a Definition of the Aurignacian, vol. 45, pp. 147–171. IPA, Lisbon.
- Boschian, G., Gerometta, K., Ellwood, B. B., & Karavanić, I. (2017). Late Neandertals in Dalmatia: Site formation processes, chronology, climate change and human activity at Mujina Pećina, Croatia. *Quaternary International*, 450, 12–35. <https://doi.org/10.1016/j.quaint.2016.09.066>
- Broglio, A., & Dalmeri, G. (2005). Pitture paleolitiche nelle Prealpi Venete: Grotta di Fumane e Riparo Dalmeri. Memorie del Museo Civico di Storia Naturale di Verona, 2a serie, Sezione Scienze dell'Uomo, 9. Verona
- Broglio, A., Bertola, S., De Stefani, M., Marini, D., Lemorini, C., & Rossetti, P. (2005). La production lamellaire et les armatures lamellaires de l'Aurignacien ancien de la grotte de Fumane (Monts Lessini, Vénétie). In F. Le Brun-Ricalens (ed.): Productions lamellaires attribuées à l'Aurignacien, pp. 415–436. MNHA, Luxembourg.
- Broglio, A., Bertola, S., De Stefani, M., & Gurioli, F. (2006). Le structure d'abitato aurignaziane della Grotta di Fumane. *Dialektikē, Cahiers de Typologie analytique*: 27–43
- Butzer, K. W. (1982). Archaeology as human ecology: Method and theory for a contextual approach. Cambridge University Press, Cambridge. <https://doi.org/10.1017/CBO9780511558245>
- Cascalheira, J. (2019). Territoriality and the organization of technology during the Last Glacial Maximum in southwestern Europe. *PLoS One*, 14, e0225828. <https://doi.org/10.1371/journal.pone.0225828>
- Clarkson, C. (2013). Measuring core reduction using 3D flake scar density: A test case of changing core reduction at Klasies River Mouth, South Africa. *Journal of Archaeological Science*, 40, 4348–4357. <https://doi.org/10.1016/j.jas.2013.06.007>
- Conard, N. J., & Bolus, M. (2006). The Swabian Aurignacian and its place in European Prehistory. In Bar-Josef, O., & Zilhão, J. (eds.): Towards a definition of the Aurignacian, pp. 219–239. IPA, Lisbon.
- Cotterell, B., & Kamminga, J. (1987). The formation of flakes. *American Antiquity*, 52, 675–708. <https://doi.org/10.2307/281378>
- Cziesla, E. (1987). L'analyse des raccords ou le concept du dynamisme en préhistoire. *Bulletin De La Société Préhistorique Du Luxembourg*, 9, 77–111.
- Cziesla, E., et al. (1990). On refitting of stone artefacts. In E. Cziesla, S. Eickhoff, & N. Arts et al. (Eds.), *The Big Puzzle: International symposium on refitting stone artefacts*, Monrepos (pp. 9–44). Bonn: Holos.
- De Stefani, M. (2003). Contributo alla conoscenza del comportamento tecnologico dell'uomo moderno nel Paleolitico Superiore: la produzione laminare nell'Aurignaziano e nel Gravettiano. Ph.D. Dissertation, University of Bologna.
- de Sonneville-Bordes, D. (1960). *Le Paléolithique supérieur en Périgord*. Bordeaux: Delmas.
- Delpiano, D., Heasley, K., & Peresani, M. (2018). Assessing Neanderthal land use and lithic raw material management in Discoid technology. *Journal of Anthropological Sciences*, 31, 89–110. <https://doi.org/10.4436/JASS.96006>
- Demars, P.-Y., & Laurent, P. (1992). Types d'outils lithiques du Paléolithique supérieur en Europe. Cahiers du Quaternaire, vol 14. CNRS, Paris
- Deschamps, M., & Zilhão, J. (2018). Assessing site formation and assemblage integrity through stone tool refitting at Gruta da Oliveira (Almonda karst system, Torres Novas, Portugal): A Middle Paleolithic case study. *PLoS One*, 13, e0192423. <https://doi.org/10.1371/journal.pone.0192423>
- Diggle, P. (2003). *Statistical analysis of spatial point patterns*. Hodder Arnold.
- Dinnis, R., Bessudnov, A., Chiotti, L., Flas, D., & Michel, A. (2019). Thoughts on the structure of the European Aurignacian, with particular focus on Hohle Fels IV. *Proceedings of the Prehistoric Society*, 85, 29–60. <https://doi.org/10.1017/ppr.2019.11>
- Discamps, E., Thomas, M., Dancette, C., Gravina, B., Plutniak, S., Royer, A., Angelin, A., Bachellerie, F., Beauval, C., Bordes, J.-G., Deschamps, M., Langlais, M., Laroulandie, V., Mallye, J.-B., Michel, A., Perrin, T., & Rendu, W. (2023). Breaking free from field layers: The interest of Post-excavation Stratigraphies (PES) for producing reliable archaeological interpretations and increasing chronological resolution. *Journal of Paleolithic Archaeology*, 6, 29. <https://doi.org/10.1007/s41982-023-00155-x>
- Douka, K., Grimaldi, S., Boschian, G., del Lucchese, A., & Higham, T. F. G. (2012). A new chronostratigraphic framework for the Upper Palaeolithic of Riparo Mochi (Italy). *Journal of Human Evolution*, 62, 286–299. <https://doi.org/10.1016/j.jhevol.2011.11.009>
- Doyon, L. (2020). The cultural trajectories of Aurignacian osseous projectile points in Southern Europe: Insights from geometric morphometrics. *Quaternary International*, 551, 63–84. <https://doi.org/10.1016/j.quaint.2018.12.010>
- Driscoll, K., & García-Rojas, M. (2014). Their lips are sealed: identifying hard stone, soft stone, and antler hammer direct percussion in Palaeolithic prismatic blade production. *Journal of Archaeological Science*, 47, 134–141. <https://doi.org/10.1016/j.jas.2014.04.008>
- Driscoll, K., Alcaina, J., Égüez, N., Mangado, X., Fullola, J.-M., & Tejero, J.-M. (2016). Trampled under foot: A quartz and chert human trampling experiment at the Cova del Parco rock shelter, Spain. *Quaternary International*, 424, 130–142. <https://doi.org/10.1016/j.quaint.2015.04.054>
- Eren, M. I., Durant, A., Neudorf, C., Haslam, M., Shipton, C., Bora, J., Korisettar, R., & Petraglia, M. (2010). Experimental examination of animal trampling effects on artifact movement in dry and water saturated substrates: A test case from South India. *Journal of Archaeological Science*, 37, 3010–3021. <https://doi.org/10.1016/j.jas.2010.06.024>
- Falcucci, A. (2018). Towards a renewed definition of the Protoaurignacian. *Mitteilungen der Gesellschaft Für Urgeschichte*, 27, 87–130.
- Falcucci, A., & Peresani, M. (2018). Protoaurignacian core reduction procedures: Blade and bladelet technologies at fumane cave. *Lithic Technology*, 43, 125–140. <https://doi.org/10.1080/0197261.2018.1439681>
- Falcucci, A., & Peresani, M. (2019). A pre-Heinrich Event 3 assemblage at Fumane Cave and its contribution for understanding the beginning of the Gravettian in Italy. *Quartär*, 66, 135–154. https://doi.org/10.7485/QU66_6
- Falcucci, A., Conard, N. J., & Peresani, M. (2017). A critical assessment of the Protoaurignacian lithic technology at Fumane Cave and its implications for the definition of the earliest Aurignacian. *PLoS One*, 12, e0189241. <https://doi.org/10.1371/journal.pone.0189241>
- Falcucci, A., Conard, N. J., & Peresani, M. (2020). Breaking through the Aquitaine frame: A re-evaluation on the significance of regional variants during the Aurignacian as seen from a key record in southern Europe. *Journal of Anthropological Sciences*, 98, 99–140. <https://doi.org/10.4436/JASS.98021>

- Falcucci, A., & Peresani, M. (2023). The Open Aurignacian Project. Volume 1: Fumane Cave in northeastern Italy (v.2.1.1). Zenodo. 10.5281/zenodo.6362149
- Falcucci, A., Arrighi, S., Spagnolo, V., Rossini, M., Higgins, O. A., Muttillo, B., Martini, I., Crezzini, J., Boschin, F., Ronchitelli, A., & Moroni, A. (2024). A pre-Campanian Ignimbrite techno-cultural shift in the Aurignacian sequence of Grotta di Castelcivita, southern Italy. *Scientific Reports*, 14, 12783. <https://doi.org/10.1038/s41598-024-59896-6>
- Farrand, W. R. (2001). Sediments and stratigraphy in rockshelters and caves: A personal perspective on principles and pragmatics. *Geoarchaeology*, 16, 537–557. <https://doi.org/10.1002/gea.1004>
- Fischer, A., Hansen, P. V., & Rasmussen, P. (1984). Macro and micro wear traces on lithic projectile points. *Journal of Danish Archaeology*, 3, 19–46. <https://doi.org/10.1080/0108464X.1984.10589910>
- Frouin, M., Douka, K., Dave, A. K., Schwenninger, J.-L., Mercier, N., Murray, A. S., Santaniello, F., Boschian, G., Grimaldi, S., & Higham, T. (2022). A refined chronology for the Middle and early Upper Paleolithic sequence of Riparo Mochi (Liguria, Italy). *Journal of Human Evolution*, 169, 103211. <https://doi.org/10.1016/j.jhevol.2022.103211>
- Gatrell, A. C., Bailey, T. C., Diggle, P. J., & Rowlingson, B. S. (1996). Spatial point pattern analysis and its application in geographical epidemiology. *Transactions of the Institute of British Geographers*, 21, 256–274. <https://doi.org/10.2307/622936>
- Gennai, J. (2021). Set in Stone? Discussing the early Upper Palaeolithic taxonomy using European and Levantine assemblages. *Materiale și Cercetări Arheologice (Serie Nouă)*, 1, 183–216. <https://doi.org/10.3406/mcarh.2021.2208>
- Giaccio, B., Hajdas, I., Isaia, R., Deino, A., & Nomade, S. (2017). High-precision 14C and 40Ar/39Ar dating of the Campanian Ignimbrite (Y-5) reconciles the time-scales of climatic-cultural processes at 40 ka. *Scientific Reports*, 7, 45940. <https://doi.org/10.1038/srep45940>
- Giusti, D., Touloukis, V., Konidaris, G., Thompson, N., Karkanas, P., Panagopoulou, E., & Harvati, K. (2018). Beyond maps: Patterns of formation processes at the Middle Pleistocene open-air site of Marathousa 1, Megalopolis basin, Greece. *Quaternary International*, 497, 137–153. <https://doi.org/10.1016/j.quaint.2018.01.041>
- Goldberg, P., Nash, D. T., & Petraglia, M. (1993). *Formation processes in archaeological context* (Vol. 17). Prehistory Press.
- Gravina, B., Bachellerie, F., Caux, S., Discamps, E., Faivre, J.-P., Galland, A., Michel, A., Teyssandier, N., & Bordes, J.-G. (2018). No reliable evidence for a Neanderthal-Châtelperronian Association at La Roche-à-Pierrot, Saint-Césaire. *Scientific Reports*, 8, 15134. <https://doi.org/10.1038/s41598-018-33084-9>
- Grimaldi, S., Porraz, G., & Santaniello, F. (2014). Raw material procurement and land use in the northern Mediterranean Arc: Insights from the first Proto-Aurignacian of Riparo Mochi (Balzi Rossi, Italy). *Quartär*, 61, 113–127. https://doi.org/10.7485/QU61_06
- Gurioli, F., Fiore, I., Tagliacozzo, G., Malerba, G., Giacobini, G., & Broglio, A. (2005). *I resti di macromammiferi del livello aurignaziano A2 della Grotta di Fumane (VR): analisi di alcune strutture d'abitato*. Pordenone: Paper presented at the IV Convegno Nazionale di Archeozoologia.
- Higham, T., Brock, F., Peresani, M., Broglio, A., Wood, R., & Douka, K. (2009). Problems with radiocarbon dating the Middle to Upper Palaeolithic transition in Italy. *Quaternary Science Reviews*, 28, 1257–1267. <https://doi.org/10.1016/j.quascirev.2008.12.018>
- Hughes, P. J., & Lampert, R. J. (1977). Occupational disturbance and types of archaeological deposit. *Journal of Archaeological Science*, 4, 135–140. [https://doi.org/10.1016/0305-4403\(77\)90060-7](https://doi.org/10.1016/0305-4403(77)90060-7)
- Inizan, M. L., Reduron, M., Roche, H., & Tixier, J. (1995). Technologie de la pierre taillée. *Préhistoire de la pierre taillée* vol Tome 4. CREP, Meudon
- Jennings, T. A. (2011). Experimental production of bending and radial flake fractures and implications for lithic technologies. *Journal of Archaeological Science*, 38, 3644–3651. <https://doi.org/10.1016/j.jas.2011.08.035>
- Kassambara, A. (2021). rstatix: Pipe-friendly framework for basic statistical tests. R package version 0.7.0. <https://CRAN.R-project.org/package=rstatix>
- Kassambara, A., & Mundt, F. (2017). Factoextra: Extract and visualize the results of multivariate data analyses. <https://cran.r-project.org/web/packages/factoextra/readme/README.html>. Accessed 8 Dec 2024.
- Laplace, G. (1977). Il Riparo Mochi ai Balzi Rossi di Grimaldi (Scavi 1939–1949). Les industries leptolithiques. *Rivista di Scienze Preistoriche*, 32, 3–131.
- Laughlin, J. P., & Kelly, R. L. (2010). Experimental analysis of the practical limits of lithic refitting. *Journal of Archaeological Science*, 37, 427–433. <https://doi.org/10.1016/j.jas.2009.10.007>
- Lê, S., Josse, J., & Husson, F. (2008). FactoMineR: An R package for multivariate analysis. *Journal of Statistical Software*, 25, 1–18. <https://doi.org/10.18637/jss.v025.i01>
- Le Brun-Ricalens, F., & Bordes, J.-G. (2007). Les débuts de l'Aurignacien en Europe Occidentale: unité ou diversité? Du territoire de subsistance au territoire culturel. In H. Floss & N. Rouquerol (Eds.), *Les chemins de l'art aurignacien en Europe*. Musée-Forum Aurignac, Aurignac: Das Aurignacien und die Anfänge der Kunst in Europa.
- Lenoble, A., & Bertran, P. (2004). Fabric of Palaeolithic levels: Methods and implications for site formation processes. *Journal of Archaeological Science*, 31, 457–469. <https://doi.org/10.1016/j.jas.2003.09.013>
- Leplongeon, A., Ménard, C., Bonhomme, V., & Bortolini, E. (2020). Backed pieces and their variability in the later Stone Age of the Horn of Africa. *African Archaeological Review*, 37, 437–468. <https://doi.org/10.1007/s10437-020-09401-x>
- Lombao, D., Falcucci, A., Moos, E., & Peresani, M. (2023). Unraveling technological behaviors through core reduction intensity. The case of the early Protoaurignacian assemblage from Fumane Cave. *Journal of Archaeological Science*, 160, 105889. <https://doi.org/10.1016/j.jas.2023.105889>
- López-García, J. M., dalla Valle, C., Cremaschi, M., & Peresani, M. (2015). Reconstruction of the Neanderthal and Modern Human landscape and climate from the Fumane cave sequence (Verona, Italy) using small-mammal assemblages. *Quaternary Science Reviews*, 128, 1–13. <https://doi.org/10.1016/j.quascirev.2015.09.013>
- Lucas, G., Rigaud, J. P., Simek, J. F., & Soressi, M. (2003). The Châtelperronian of Grotte XVI, Cénac-et-Saint-Julien (Dordogne, France). In Zilhão, J. & D'Errico, F. (eds.): The chronology of the Aurignacian and of the transitional technocomplexes. Dating, Stratigraphies, Cultural Implications, pp. 289–298. IPA, Lisboa.
- Maier, A., Schmidt, I., & Zimmermann, A. (2022). A large-scale view on ‘small-scale societies’ - Observations on population size, density, distribution, and connectedness of Upper Palaeolithic hunter-gatherers in Western and Central Europe. In T. Widlok & M. Dores Cruz (eds.): Scale Matters. The Quality of Quantity in Human Culture and Sociality, vol. 263, pp. 129–146. Transcript, Bielefeld.
- Marcazzan, D., Miller, C. E., Ligouis, B., Duches, R., Conard, N. J., & Peresani, M. (2022). Middle and Upper Paleolithic occupations of Fumane Cave (Italy): A geoarchaeological investigation of

- the anthropogenic features. *Journal of Anthropological Sciences*, 100, 1–26. <https://doi.org/10.4436/jass.10002>
- Marín-Arroyo, A. B., Terlato, G., Vidal-Cordasco, M., & Peresani, M. (2023). Subsistence of early anatomically modern humans in Europe as evidenced in the Protoaurignacian occupations of Fumane Cave. *Italy. Scientific Reports*, 13, 3788. <https://doi.org/10.1038/s41598-023-30059-3>
- Martini, I., Baucon, A., & Boschin, F. (2021). Depositional processes and environmental settings in rock shelters: The case of the prehistoric Oscurusciuto site (Southern Italy). *Geological Magazine*, 158, 891–904. <https://doi.org/10.1017/s0016756820001041>
- Marwick, B., Hayes, E., Clarkson, C., & Fullagar, R. (2017). Movement of lithics by trampling: An experiment in the Madjedbebe sediments, northern Australia. *Journal of Archaeological Science*, 79, 73–85. <https://doi.org/10.1016/j.jas.2017.01.008>
- McBrearty, S., Bishop, L., Plummer, T., Dewar, R., & Conard, N. (1998). Tools underfoot: Human trampling as an agent of lithic artifact edge modification. *American Antiquity*, 63, 108–129. <https://doi.org/10.2307/2694779>
- McPherron, S. J. P., Dibble, H. L., & Goldberg, P. (2005). *Z. Geoarchaeology*, 20, 243–262. <https://doi.org/10.1002/gea.20048>
- Miller, C. E., Conard, N. J., Goldberg, P., & Berna, F. (2010). Dumping, sweeping and trampling: Experimental micromorphological analysis of anthropogenically modified combustion features. *Paleithnologie*, 2, 25–37.
- Moreau, L., Odar, B., Higham, T., Horvat, A., Pirkmajer, D., & Turk, P. (2015). Reassessing the Aurignacian of Slovenia: Techno-economic behaviour and direct dating of osseous projectile points. *Journal of Human Evolution*, 78, 158–180. <https://doi.org/10.1016/j.jhevol.2014.09.007>
- Moroni, A., Ronchitelli, A., Arrighi, S., Aureli, D., Bailey, S., Boscato, P., Boschin, F., Capecci, G., Crezzini, J., Douka, K., Marciani, G., Panetta, D., Ranaldo, F., Scaramucci, S. S. R., Spagnolo, V., Benazzi, S., & Gambassini, P. (2018). Grotta del Cavallo (Apulia – Southern Italy). The Uluzzian in the mirror. *Journal of Anthropological Sciences*, 96, 1–36. <https://doi.org/10.4436/jass.96004>
- Nigst, P. R., Haesaerts, P., Damblon, F., Frank-Fellner, C., Mallol, C., Viola, B., Götzinger, M., Niven, L., Trnka, G., & Hublin, J.-J. (2014). Early modern human settlement of Europe north of the Alps occurred 43,500 years ago in a cold steppe-type environment. *Proceedings of the National Academy of Sciences*, 111, 14394–14399. <https://doi.org/10.1073/pnas.1412201111>
- Normand, C. (2006). L'Aurignacien de la salle de Saint-Martin (Grotte d'Isturitz, commune de Saint-Martin d'Arberoue, Pyrénées-atlantiques): donnés préliminaires sur l'industrie lithique recueillie lors des campagnes 2000–2002. In F. Bon, J.M. Maillo Fernández, & D. Ortega-Cobos (Eds.), Autour des concepts de Proto-aurignacien, d'Aurignacien archaïque, initial et ancien. Unité et variabilité des comportements techniques des premiers groupes d'hommes modernes dans le sud de la France et le nord de l'Espagne (pp. 145–174). UNED, Madrid.
- Oksanen, J., Simpson, G., Blanchet, F., Kindt, R., Legendre, P., Minchin, P., O'Hara, R., Sølymos, P., Stevens, M., Szoecs, E., Wagner, H., Barbour, M., Bedward, M., Bolker, B., Borcard, D., Carvalho, G., Chirico, M., De Caceres, M., Durand, S., Evangelista, H., FitzJohn, R., Friendly, M., Furneaux, B., Hannigan, G., Hill, M., Lahti, L., McGlinn, D., Ouellette, M., Ribeiro Cunha, E., Smith, T., Stier, A., Ter Braak, C., & Weedon, J. (2022). *vegan: Community Ecology Package*. R package version 2.6–2. <https://CRAN.R-project.org/package=vegan>. Accessed 8 Dec 2024.
- Pelegrin, J. (1995). *Technologie lithique: Le Chatelperronian de Roc-de-Combe (lot) et de La Cote (Dordogne)*. CNRS Editions.
- Peresani, M. (2012). Fifty thousand years of flint knapping and tool shaping across the Mousterian and Uluzzian sequence of Fumane cave. *Quaternary International*, 247, 125–150. <https://doi.org/10.1016/j.quaint.2011.02.006>
- Peresani, M. (2022). Inspecting human evolution from a cave. Late Neanderthals and early sapiens at Grotta di Fumane: Present state and outlook. *Journal of Anthropological Sciences*, 100, 71–107. <https://doi.org/10.4436/jass.10016>
- Peresani, M., Cristiani, E., & Romandini, M. (2016). The Uluzzian technology of Grotta di Fumane and its implication for reconstructing cultural dynamics in the Middle–Upper Palaeolithic transition of Western Eurasia. *Journal of Human Evolution*, 91, 36–56. <https://doi.org/10.1016/j.jhevol.2015.10.012>
- Peresani, M., Forte, M., Quaggiotto, E., Colonese, A. C., Romandini, M., Cilli, C., & Giacobini, G. (2019a). Marine and freshwater shell exploitation in the Early Upper Paleolithic: Re-examination of the assemblages from Fumane Cave (NE Italy). *PaleoAnthropology*, 2019, 64–81. <https://doi.org/10.4207/PA.2019.ART124>
- Peresani, M., Bertola, S., Delpiano, D., Benazzi, S., & Romandini, M. (2019b). The Uluzzian in the north of Italy: Insights around the new evidence at Riparo Broion. *Archaeological and Anthropological Sciences*, 11, 3503–3536. <https://doi.org/10.1007/s12520-018-0770-z>
- Peretto, C., Biagi, P., Boschian, G., Broglio, A., De Stefani, M., Fasani, L., Fontana, F., Grifoni, R., Guerreschi, A., Iacopini, A., Minelli, A., Pala, F., Peresani, M., Radi, G., Ronchitelli, A., Sarti, L., Thun-Hohenstein, U., & Tozzi, C. (2004). Living-floors and structures from the Lower Palaeolithic to the Bronze Age. *Collegium Antropologicum*, 28, 63–88.
- Posit team. (2023). *RStudio: Integrated development environment for R*. PBC, Boston, MA: Posit Software.
- R Core team. (2022). *R: A language and environment for statistical computing*. R Foundation for statistical computing, Vienna. <https://www.R-project.org/>. Accessed 8 Dec 2024.
- Riel-Salvatore, J., & Negrino, F. (2018a). Human adaptations to climatic change in Liguria across the Middle–Upper Paleolithic transition. *Journal of Quaternary Science*, 33, 313–322. <https://doi.org/10.1002/jqs.3005>
- Riel-Salvatore, J., & Negrino, F. (2018b). Proto-Aurignacian lithic technology, mobility, and human niche construction: A case study from Riparo Bombrini. In E. Robinson & F. Sellet (Eds.), *Lithic technological organization and paleoenvironmental change* (pp. 163–187). NY: Springer.
- Roche, H., & Tixier, J. (1982). Les accidents de taille. *Studia Praehistorica Belgica*, 2, 65–76.
- Romagnoli, F., & Vaquero, M. (2019). The challenges of applying refitting analysis in the Palaeolithic archaeology of the twenty-first century: An actualised overview and future perspectives. *Archaeological and Anthropological Sciences*, 11, 4387–4396. <https://doi.org/10.1007/s12520-019-00888-3>
- Romagnoli, F., Nishiaki, Y., Rivals, F., & Vaquero, M. (2018). Time uncertainty, site formation processes, and human behaviours: New insights on old issues in High-Resolution Archaeology. *Quaternary International*, 474, 99–102. <https://doi.org/10.1016/j.quaint.2018.04.033>
- Roussel, M., Bourguignon, L., & Soressi, M. (2009). Identification par l'expérimentation de la percussion au percuteur de calcaire au Paléolithique moyen : le cas du façonnage des racloirs bifaciaux Quina de Chez Pinaud (Jonzac, Charente-Maritime). *Bulletin de la Société préhistorique française*, 106, 219–238.
- Roussel, M., Soressi, M., & Hublin, J. J. (2016). The Chatelperronian conundrum: Blade and bladelet lithic technologies from Quincay, France. *Journal of Human Evolution*, 95, 13–32. <https://doi.org/10.1016/j.jhevol.2016.02.003>
- Santamaría, D. (2012). La transición del Paleolítico medio al superior en Asturias. El Abrigo de La Viña (La Manzaneda, Oviedo) y la Cueva de El Sidrón (Borines, Piloña). Ph.D. Dissertation, Universidad de Oviedo.

- Sánchez-Romero, L., Benito-Calvo, A., Iriarte, E., Emeterio, A. S., Ortega, I., & Ríos-Garaizar, J. (2022). Unraveling Châtelperronian high-density accumulations: The open-air site of Aranbaltza II (Bizkaia, Spain). *Archaeological and Anthropological Sciences*, 14, 77. <https://doi.org/10.1007/s12520-022-01541-2>
- Scerri, E. M. L., Drake, N. A., Jennings, R., & Groucutt, H. S. (2014). Earliest evidence for the structure of *Homo sapiens* populations in Africa. *Quaternary Science Reviews*, 101, 207–216. <https://doi.org/10.1016/j.quascirev.2014.07.019>
- Schiffer, M. B. (1987). *Formation processes of the archaeological record*. University of New Mexico Press.
- Sigari, D., Zangrossi, F., & Peresani, M. (2022). New ochre painted stones from the late ProtoAurignacian of Fumane Cave. *Anthropologie*, LX, 453–468. <https://doi.org/10.26720/anthro.22.03.03.1>
- Sisk, M. L., & Shea, J. J. (2008). Intrisite spatial variation of the Omo Kibish Middle Stone Age assemblages: Artifact refitting and distribution patterns. *Journal of Human Evolution*, 55, 486–500. <https://doi.org/10.1016/j.jhevol.2008.05.016>
- Strobl, J., & Obermaier, H. (1909). Die Aurignaciens-Station von Krems (N.-Ö.). *Jahrbuch Für Altertumskunde*, III, 129–148.
- Talamo, S., Soressi, M., Roussel, M., Richards, M., & Hublin, J.-J. (2012). A radiocarbon chronology for the complete Middle to Upper Palaeolithic transitional sequence of Les Cottés (France). *Journal of Archaeological Science*, 39, 175–183. <https://doi.org/10.1016/j.jas.2011.09.019>
- Tejero, J. M., & Grimaldi, S. (2015). Assessing bone and antler exploitation at Riparo Mochi (Balzi Rossi, Italy): Implications for the characterization of the Aurignacian in South-western Europe. *Journal of Archaeological Science*, 61, 59–77. <https://doi.org/10.1016/j.jas.2015.05.003>
- Texier, J. (2000). A propos des processus de formation des sites préhistoriques / About prehistoric site formation processes. *Paléo, Revue D'archéologie Préhistorique*, 12, 379–386.
- Teyssandier, N., & Zilhão, J. (2018). On the entity and antiquity of the Aurignacian at Willendorf (Austria): Implications for modern human emergence in Europe. *Journal of Paleolithic Archaeology*, 1, 107–138. <https://doi.org/10.1007/s41982-017-0004-4>
- Thomas, M., Discamps, E., Gravina, B., & Texier, J.-P. (2019). Analyse taphonomique et spatiale de palimpsestes d'occupations moustériennes de l'abri inférieur du Moustier (Dordogne, France). *PALEO : Revue D'archéologie Préhistorique*, 30, 278–299. <https://doi.org/10.4000/paleo.4897>
- Tixier, J. (1963). *Typologie de l'Epipaléolithique du Maghreb* (Vol. 2). Mémoires du Centre de Recherches anthropologiques et préhistoriques et ethnographiques.
- Tostevin, G. (2013). *Seeing lithics: A Middle-Range Theory for testing for cultural transmission in the Pleistocene*. Oxbow Books.
- Tsanova, T. (2008). Les débuts du Paléolithique supérieur dans l'Est des Balkans. Réflexion à partir de l'étude taphonomique et technicoéconomique des ensembles lithiques de Bacho Kiro (couche 11), Temnata (couches VI et 4) et Kozarnika (niveau VII). vol 1752. BAR International Series Oxford.
- Tsanova, T. (2013). The beginning of the Upper Paleolithic in the Iranian Zagros. A taphonomic approach and techno-economic comparison of Early Baradostian assemblages from Warwasi and Yafteh (Iran). *Journal of Human Evolution*, 65, 39–64. <https://doi.org/10.1016/j.jhevol.2013.04.005>
- Vanhaeren, M., & d'Errico, F. (2006). Aurignacian ethno-linguistic geography of Europe revealed by personal ornaments. *Journal of Archaeological Science*, 33, 1105–1128. <https://doi.org/10.1016/j.jas.2005.11.017>
- Vaquero, M., Fernández-Laso, M. C., Chacón, M. G., Romagnoli, F., Rosell, J., & Sañudo, P. (2017). Moving things: Comparing lithic and bone refits from a Middle Paleolithic site. *Journal of Anthropological Archaeology*, 48, 262–280. <https://doi.org/10.1016/j.jaa.2017.09.001>
- Vaquero, M., Romagnoli, F., Bargalló, A., Chacón, M. G., Gómez de Soler, B., Picin, A., & Carbonell, E. (2019). Lithic refitting and intrasite artifact transport: A view from the Middle Paleolithic. *Archaeological and Anthropological Sciences*, 11, 4491–4513. <https://doi.org/10.1007/s12520-019-00832-5>
- Villa, P. (1982). Conjoinable pieces and site formation processes. *American Antiquity*, 47, 276–290. <https://doi.org/10.2307/279901>
- Villa, P. (2004). Taphonomy and stratigraphy in European prehistory. *Before Farming*, 2004/1, 1–20.
- Villa, P., & Courtin, J. (1983). The interpretation of stratified sites: A view from underground. *Journal of Archaeological Science*, 10, 267–281. [https://doi.org/10.1016/0305-4403\(83\)90011-0](https://doi.org/10.1016/0305-4403(83)90011-0)
- Weitzel, C., & Sánchez, A. (2021). A trampling experiment to assess fractures and edge damage in Quarry's lithic assemblages. *Lithic Technology*, 46, 286–301. <https://doi.org/10.1080/01977261.2021.1926702>
- Wickham, H., Averick, M., Bryan, J., Chang, W., McGowan, L. D., François, R., Grolemund, G., Hayes, A., Henry, L., Hester, J., Kuhn, M., Pedersen, T. L., Miller, E., Bache, S. M., Müller, K., Ooms, J., Robinson, D., Seidel, D. P., Spinu, V., & Yutani, H. (2019). Welcome to the Tidyverse. *Journal of Open Source Software*, 4, 1686. <https://doi.org/10.21105/joss.01686>
- Wood, R. E., Arrizabalaga, A., Camps, M., Fallon, S., Iriarte-Chiapuso, M. J., Jones, R., Maroto, J., de la Rasilla, M., Santamaría, D., Soler, J., Soler, N., Villaluenga, A., & Higham, T. (2014). The chronology of the earliest Upper Palaeolithic in northern Iberia: New insights from L'Arbreda, Labeko Koba and La Viña. *Journal of Human Evolution*, 69, 91–109. <https://doi.org/10.1016/j.jhevol.2013.12.017>
- Zilhão, J., d'Errico, F., Banks, W. E., & Teyssandier, N. (2024). A Data-Driven Paradigm Shift for the Middle-to-Upper Palaeolithic Transition and the Neandertal Debate. *Quaternary Environments and Humans*, 100037. <https://doi.org/10.1016/j.qeh.2024.100037>

Publisher's Note Springer Nature remains neutral with regard to jurisdictional claims in published maps and institutional affiliations.